



# Analysis of low-energy response and possible emergent SU(4) Kondo state in a double quantum dot

Yunori Nishikawa,<sup>1,2</sup> Alex C. Hewson,<sup>2</sup> Daniel J. G. Crow,<sup>2</sup> and Johannes Bauer<sup>3</sup>

<sup>1</sup>*Department of Physics, Osaka City University, Sumiyoshi-ku, Osaka 558-8585, Japan*

<sup>2</sup>*Department of Mathematics, Imperial College, London SW7 2AZ, UK*

<sup>3</sup>*Department of Physics, Harvard University, Cambridge, Massachusetts 02138, USA*

(Received 25 September 2013; published 26 December 2013)

We examine the low-energy behavior of a double quantum dot in a regime where spin and pseudospin excitations are degenerate. The individual quantum dots are described by Anderson impurity models with an on-site interaction  $U$  which are capacitively coupled by an interdot interaction  $U_{12} < U$ . The low-energy response functions are expressed in terms of renormalized parameters, which can be deduced from an analysis of the fixed point in a numerical renormalization group calculation. At the point where the spin and pseudospin degrees of freedom become degenerate, the free quasiparticle excitations have a phase shift of  $\pi/4$  and a 4-fold degeneracy. We find, however, when the quasiparticle interactions are included, that the low-energy effective model has SU(4) symmetry only in the special case  $U_{12} = U$  unless both  $U$  and  $U_{12}$  are greater than  $D$ , the half bandwidth of the conduction electron bath. We show that the gate voltage dependence of the temperature-dependent differential conductance observed in recent experiments can be described by a quasiparticle density of states with temperature-dependent renormalized parameters.

DOI: [10.1103/PhysRevB.88.245130](https://doi.org/10.1103/PhysRevB.88.245130)

PACS number(s): 73.21.La, 72.15.Qm, 75.20.Hr, 72.10.Fk

## I. INTRODUCTION

There has been much recent theoretical and experimental interest in the low-energy behavior of coupled quantum dots where the electrons are strongly confined on the dots.<sup>1–10</sup> As a consequence of this confinement, the on-site and intersite interactions between the electrons on the dots are strong and their coupling to their environmental electron baths relatively weak. Such systems can be used to probe the effects of strong local electron correlation, such as the Kondo effect, in great detail.<sup>11–15</sup> Experimentally it is possible to vary many of the parameters in these nanoscale systems in a controlled way; for example, the energy levels on the dots can be changed through the application of individual gate voltages to the dots making it possible to investigate different parameter regimes. Strong correlation behavior in steady-state nonequilibrium conditions can be examined by applying bias voltages to the individual dots and then measuring the electron transport through the dots. Borda *et al.*<sup>3</sup> have drawn attention to the situation of a singly occupied double quantum dot where the spin and interdot excitations are degenerate. The interdot charge fluctuations can be interpreted as pseudospin fluctuations, the occupation of one dot by a single electron corresponding to an “up” pseudospin, and the single occupation of the other dot to a “down” pseudospin. On the basis of scaling equations for an effective Kondo model it was concluded that, in this regime, a new symmetry would emerge on a low-energy scale between the spin and pseudospin excitations, such that the low-energy behavior could be described by an effective model with SU(4) symmetry.<sup>3,16–19</sup>

Recently it has proved possible to realize this situation experimentally using two capacitively coupled dots,<sup>20–22</sup> and to measure the response to an effective pseudospin field by changing the levels on the dots. The conductance of the electrons through the individual dots has also been measured, offering the potential to examine the theoretical predictions in detail. One technique for calculating the low-energy behavior is via the determination of the renormalized parameters which

specify the effective Hamiltonian in this regime. These can be determined from an analysis of the low-energy fixed point in a numerical renormalization group (NRG) calculation.<sup>23–26</sup> Once these have been determined several response functions, such as the spin and charge susceptibilities at zero temperature and the linear conductance through the dots, can be calculated from exact expressions for these quantities in terms of these renormalized parameters. By comparing with exact Bethe ansatz results it has been shown that very accurate numerical results can be obtained from these calculations.<sup>25,27,28</sup> Furthermore leading order corrections to some of these results can be determined exactly using these parameters within a renormalized perturbation theory (RPT).<sup>29</sup> We use this technique in this paper to examine the circumstances in which the low-energy behavior could correspond to an SU(4) model due to degenerate spin and interdot (orbital) fluctuations. We calculate the spin and orbital susceptibilities and look at the effect of introducing a magnetic field to suppress the spin fluctuations and induce a crossover to an SU(2) pseudospin Kondo effect. Finally we estimate temperature dependence of the linear conductance in terms of temperature-dependent parameters for the quasiparticles, and show that this approach gives results in line with recent experimental observations.

## II. MODEL HAMILTONIAN

The Hamiltonian for the double quantum dot can be expressed in the form

$$H = \sum_{i=1,2} (H_{d,i} + H_{\text{bath},i} + H_{c,i}) + H_{12}, \quad (1)$$

where  $H_{d,i}$  describes the individual dots,  $i = 1, 2$ ,  $H_{\text{bath},i}$  the baths to which the dots are individually coupled by a coupling term  $H_{c,i}$ , and  $H_{12}$  is the interaction between the dots. A reasonable approximation is to take the baths, two for each

dot, to be described by a free electron model,

$$H_{\text{bath},i} = \sum_{k,\alpha,\sigma} \varepsilon_k c_{k,i,\alpha,\sigma}^\dagger c_{k,i,\alpha,\sigma}, \quad (2)$$

where  $\alpha = s, d$  (source, drain) and  $\varepsilon_k$  is an energy level in a bath, taken to be independent of  $\alpha, i$ , and  $\sigma$ .

The Hamiltonian describing the dots  $H_{d,i}$  is taken in the form

$$H_{d,i} = \sum_{\sigma} \varepsilon_{d,i,\sigma} c_{d,i,\sigma}^\dagger c_{d,i,\sigma} + U_i n_{d,i,\uparrow} n_{d,i,\downarrow}, \quad (3)$$

where  $\varepsilon_{d,i,\sigma}$  is the level position on dot  $i$  in a magnetic field  $h$ ,  $\varepsilon_{d,i,\sigma} = \varepsilon_{d,i} - \sigma h$ , relative to the chemical potential  $\mu_i$ , and  $U_i$  is the intradot interaction. It will be useful to introduce an analogous pseudospin field  $h_{\text{ps}}$  by writing  $\varepsilon_{d,1} = \bar{\varepsilon}_d - h_{\text{ps}}$  and  $\varepsilon_{d,2} = \bar{\varepsilon}_d + h_{\text{ps}}$ , where  $\bar{\varepsilon}_d = 0.5(\varepsilon_{d,1} + \varepsilon_{d,2})$ .

The coupling of the dots to the leads is described by a hybridization term,

$$H_{c,i} = \sum_{k,\alpha,\sigma} V_{k,i,\alpha} (c_{k,i,\alpha,\sigma}^\dagger c_{d,i,\sigma} + \text{H.c.}). \quad (4)$$

We will assume no energy dependence of the matrix elements but allow them to differ in the different channels. We define the widths  $\Gamma_{i,\alpha} = \pi V_{i,\alpha}^2 \rho_c(0)$  with the conduction electron density of states  $\rho_c$  as the constant energy scale for hybridization, and their sum,  $\Gamma_i = \sum_{\alpha} \Gamma_{i,\alpha}$ . For transport close to equilibrium only the combination  $V_{i,s} c_{k,i,s,\sigma}^\dagger + V_{i,d} c_{k,i,d,\sigma}^\dagger$  couples to the dot states. We can therefore simplify the problem to two dots and two itinerant channels.

Finally for the coupling between the two dots we assume a hopping term  $t$  and a repulsive interaction between the charges on each dot  $U_{12}$ ,

$$H_{12} = t \sum_{\sigma} (c_{d,1,\sigma}^\dagger c_{d,2,\sigma} + \text{H.c.}) + U_{12} \sum_{\sigma,\sigma'} n_{d,1,\sigma} n_{d,2,\sigma'}. \quad (5)$$

To get an idea of the order of magnitude of these parameters we quote values estimated in recent experimental work:<sup>21</sup>  $U_1 \approx 1.2$  meV,  $U_2 \approx 1.5$  meV,  $U_{12} \approx 0.1$  meV,  $\Gamma_1, \Gamma_2 \approx 0.005\text{--}0.02$  meV, and  $t \sim 0$ . Due to the very small value of the hopping term  $t$  we will neglect this term in the calculations presented here.

The ground-state electron configurations for the isolated double-dot system for the Hamiltonian Eq. (1) with the occupation numbers  $[n_{d,1}, n_{d,2}]$  as functions of on-site energy  $\bar{\varepsilon}_d$  and pseudospin field  $h_{\text{ps}}$  are shown in Fig. 1.<sup>1</sup> Note that in an experiment  $\varepsilon_d$  can be tuned via gate voltages.<sup>20–22</sup>

### III. THE LOW-ENERGY EFFECTIVE MODEL

The low-energy fixed point of this model corresponds to a Fermi liquid theory and we can, therefore, assume that the self-energy  $\Sigma_{i,\sigma}(\omega)$  for the single-electron Green's function on dot  $i$  is nonsingular at  $\omega = 0$ . We can hence describe the low-energy behavior in terms of well-defined quasiparticles and their interactions. We have shown in earlier work<sup>25,26</sup> in the absence of a magnetic field that these quasiparticles can be taken to correspond to renormalized versions of the parameters that specify the bare model,  $\tilde{\varepsilon}_{d,i,\sigma}$ ,  $\tilde{\Gamma}_i$ ,  $\tilde{U}_i$ , and  $\tilde{U}_{12}$ . The Hamiltonian describing the low-energy fixed point and the leading irrelevant correction terms then has the same form as

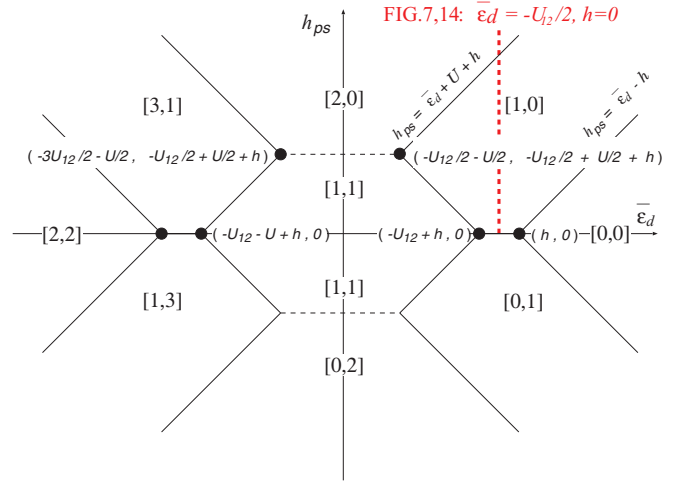


FIG. 1. (Color online) The ground-state electron configurations of the isolated double dot in  $(\bar{\varepsilon}_d, h_{\text{ps}})$  plane at a magnetic field  $h (\geq 0)$ . The meaning of  $[n_{d,1}, n_{d,2}]$  in the figure is that the number of electrons on dot  $i$  ( $i = 1, 2$ ) is  $n_{d,i}$ .

the original model, but with the bare parameters replaced by the renormalized ones. The interaction terms have to be normal ordered as they only come into play when two or more single-particle excitations are created from the interacting ground state. In the presence of a magnetic field the interdot interaction in the low-energy effective Hamiltonian has to be generalized to the form

$$\sum_{\sigma,\sigma'} \tilde{U}_{12}^{\sigma,\sigma'} :n_{d,1,\sigma} n_{d,2,\sigma'}:, \quad (6)$$

to allow for the fact that the quasiparticle interactions can be spin dependent, where the brackets  $: \hat{O} :$  indicate a normal ordering of the operator  $\hat{O}$ .

More generally a renormalized form of perturbation theory can be formulated in terms of these quasiparticles<sup>29–31</sup> in which all interaction terms of the bare model are included. This requires the explicit taking into account of counter terms to avoid overcounting renormalization effects which have already been included in the use of renormalized parameters. For simplicity we will assume the dots to be identical, apart from the energy levels  $\varepsilon_{i,\sigma}$ , so  $\Gamma_i = \Gamma$  and  $U_i = U$  and the corresponding renormalized parameters will be taken to be independent of  $i$ .

Before calculating the renormalized parameters we consider a number of quantities that can be expressed exactly in terms of these parameters. The linear coefficient of the specific-heat coefficient  $\gamma$  due to the dots is independent of the quasiparticle interactions, as expected in a Fermi liquid theory, and is given by

$$\gamma = \frac{\pi^2 \sum_{i,\sigma} \tilde{\rho}_{i,\sigma}(0)}{3}, \quad (7)$$

where  $\tilde{\rho}_{i,\sigma}(\omega)$  is the free quasiparticle density of states per single spin and channel,

$$\tilde{\rho}_{i,\sigma}(\omega) = \frac{\tilde{\Gamma}/\pi}{(\omega - \tilde{\varepsilon}_{d,i,\sigma})^2 + \tilde{\Gamma}^2}. \quad (8)$$

Here  $\tilde{\Gamma} = z\Gamma$ , where  $z$  is quasiparticle weight factor. The phase shift  $\delta_{i,\sigma}$  per spin on the dot connected to channel  $i$  is given by the Friedel sum rule,

$$\delta_{i,\sigma} = \frac{\pi}{2} - \tan^{-1} \left( \frac{\varepsilon_{d,i,\sigma} + \Sigma_{i,\sigma}(0)}{\Gamma} \right), \quad (9)$$

and equivalently in terms of the renormalized parameters,

$$\delta_{i,\sigma} = \frac{\pi}{2} - \tan^{-1} \left( \frac{\tilde{\varepsilon}_{d,i,\sigma}}{\tilde{\Gamma}} \right). \quad (10)$$

The total occupation of the impurity sites  $n_{d,\text{tot}}$  is given by  $n_{d,\text{tot}} = \sum_{i,\sigma} n_{d,i,\sigma} = \sum_{i,\sigma} \delta_{i,\sigma} / \pi$  at  $T = 0$ . These expressions in terms of renormalized parameters already allow us to draw first conclusions about the occurrence of an emergent SU(4) symmetry. If, in the absence of an applied magnetic field,  $\tilde{\varepsilon}_{d,i} = \tilde{\varepsilon}_d = \tilde{\Gamma}$  for  $i = 1, 2$  we have level degeneracy on the dots  $\tilde{\varepsilon}_{d,1} = \tilde{\varepsilon}_{d,2}$ , so  $\tilde{\rho}_1(0) = \tilde{\rho}_2(0) = \tilde{\rho}(0) = 1/2\pi\tilde{\Gamma}$ , and the phase shifts per spin per dot are all equal to  $\pi/4$ . Hence at the free quasiparticle level the system in this regime has SU(4) symmetry. However, the quasiparticle interaction terms play an important role in determining the low-energy behavior. They correspond to the leading correction terms to the fixed point, and so the low-energy model only has SU(4) symmetry if this symmetry is retained when these terms are included.

Other exact equations are for the total charge susceptibility,<sup>26</sup>

$$\chi_c = \sum_{\sigma} [\tilde{\eta}_{c,1,\sigma} \tilde{\rho}_{1,\sigma}(0) + \tilde{\eta}_{c,2,\sigma} \tilde{\rho}_{2,\sigma}(0)], \quad (11)$$

where the term  $\tilde{\eta}_{c,i,\sigma}$  takes into account the quasiparticle interactions and is given by

$$\tilde{\eta}_{c,i,\sigma} = 1 - \tilde{U} \tilde{\rho}_{i,-\sigma}(0) - \sum_{i' \neq i, \sigma'} \tilde{U}_{12}^{\sigma, \sigma'} \tilde{\rho}_{i', \sigma'}(0). \quad (12)$$

In the case with level degeneracy on the dots and no external magnetic field, we can expect the total charge susceptibility to be negligible if  $U/\pi\Gamma \gg 1$  and  $U_{12}/\pi\Gamma \gg 1$ . This is because double occupancy on a single dot is inhibited by the large value of  $U$  and double occupation of the two dots with one electron on each dot is inhibited by the large value of  $U_{12}$ . Equating the total charge susceptibility to zero at this degeneracy point gives a relation between the renormalized parameters,

$$\tilde{U} + 2\tilde{U}_{12} = 2\pi\tilde{\Gamma}. \quad (13)$$

Away from this degeneracy point, if the ground state of the system has on average one electron on the two dots, and  $U/\pi\Gamma \gg 1$  and  $U_{12}/\pi\Gamma \gg 1$ , then we still expect the charge susceptibility to be negligible and we get a more general condition,

$$\sum_{i=1,2} \tilde{\rho}_i(0) [1 - \tilde{U} \tilde{\rho}_i(0)] - 4\tilde{U}_{12} \tilde{\rho}_1(0) \tilde{\rho}_2(0) = 0. \quad (14)$$

The total spin susceptibility,  $\chi_s = \sum_i dm_i/dh$ ,  $m_i = (n_{d,i,\uparrow} - n_{d,i,\downarrow})/2$ , of the two dots is given by<sup>26</sup>

$$\chi_s = \sum_{\sigma} [\tilde{\eta}_{s,1,\sigma} \tilde{\rho}_{1,\sigma}(0) + \tilde{\eta}_{s,2,\sigma} \tilde{\rho}_{2,\sigma}(0)], \quad (15)$$

where

$$\tilde{\eta}_{s,i,\sigma} = 1 + \tilde{U} \tilde{\rho}_{i,-\sigma}(0), \quad (16)$$

and the pseudospin susceptibility,  $\chi_{\text{ps}} = dm_{\text{ps}}/dh_{\text{ps}}$ ,  $m_{\text{ps}} = (n_{d,1} - n_{d,2})/2$ , by

$$\chi_{\text{ps}} = \sum_{\sigma} [\tilde{\eta}_{\text{ps},1,\sigma} \tilde{\rho}_{1,\sigma}(0) + \tilde{\eta}_{\text{ps},2,\sigma} \tilde{\rho}_{2,\sigma}(0)], \quad (17)$$

where  $\tilde{\eta}_{\text{ps},i,\sigma}$  is given by

$$\tilde{\eta}_{\text{ps},i,\sigma} = 1 - \tilde{U} \tilde{\rho}_{i,-\sigma}(0) + \sum_{i' \neq i, \sigma'} \tilde{U}_{12}^{\sigma, \sigma'} \tilde{\rho}_{i', \sigma'}(0). \quad (18)$$

At the degeneracy point in the absence of a magnetic field these become

$$\chi_s = \frac{1}{\pi\tilde{\Gamma}} \left( 1 + \frac{\tilde{U}}{2\pi\tilde{\Gamma}} \right), \quad (19)$$

and for the pseudospin

$$\chi_{\text{ps}} = \frac{1}{\pi\tilde{\Gamma}} \left( 1 + \frac{2\tilde{U}_{12} - \tilde{U}}{2\pi\tilde{\Gamma}} \right). \quad (20)$$

For SU(4) symmetry of the effective Hamiltonian with renormalized parameters determining the low-energy behavior at this degeneracy point we require  $\tilde{U}_{12} = \tilde{U}$ , which as expected makes the spin and pseudospin susceptibilities equal. From Eq. (13) this implies  $\tilde{U}_{12} = 2\pi\tilde{\Gamma}/3 = \tilde{U}$ , giving the known Wilson ratio,  $W_s = \pi^2 \chi_s / (3\gamma)$ , for an SU(4) Kondo model of 4/3. We have only one energy scale in this case which will be the Kondo temperature  $T_K$  for the SU(4) Kondo model which we can define by the relation

$$4T_K = \frac{1}{\tilde{\rho}(0)} = \pi\tilde{\Gamma} \left( 1 + \frac{\tilde{\varepsilon}_d^2}{\tilde{\Gamma}^2} \right) = 2\pi\tilde{\Gamma}, \quad (21)$$

where for the last equation the degeneracy point was assumed.

If we raise the spin degeneracy by an applied magnetic field but keep the average electron occupation on each dot as 1/2, and  $\rho_{1,\sigma}(0) = \rho_{2,\sigma}(0)$ , then eventually in a large magnetic field we will be left with only one spin type on each dot. We take this to correspond to spin up so that in this limit,  $\rho_{i,\downarrow}(0) \rightarrow 0$ . For magnetic field energies small compared with both  $U_{12}$  and  $U$ , we can still equate the charge susceptibility to zero, which would imply  $\rho_{i,\uparrow}(0) \rightarrow 1/\pi\tilde{\Gamma}$ . There is then no enhancement of the spin susceptibility, but an enhancement of the pseudospin susceptibility by a factor  $1 + \tilde{U}_{12}/\pi\tilde{\Gamma}$  corresponding to a pseudospin Kondo effect. For  $U_{12} \gg \pi\Gamma$ , we have  $\tilde{U}_{12}/\pi\tilde{\Gamma} \rightarrow 1$  giving the SU(2) pseudospin Wilson ratio  $W_{\text{ps}} = \pi^2 \chi_{\text{ps}} / (3\gamma) = 2$ .

To test these relations, and more generally evaluate spin and pseudospin susceptibilities as a function of the energy levels on the dot and applied magnetic field, we need to calculate the renormalized parameters. We describe briefly in Appendix A how these can be deduced from an analysis of the low-energy fixed point in a numerical renormalization group (NRG) calculation.<sup>25,26</sup> We apply the method to the model being investigated here and describe the results of these calculations in detail in the next section. We typically retain 4000 states in our NRG calculations and use  $\Lambda = 6$ . This comparatively large value gives accurate estimates for the renormalized parameters as can be checked in the case of a single-impurity model.

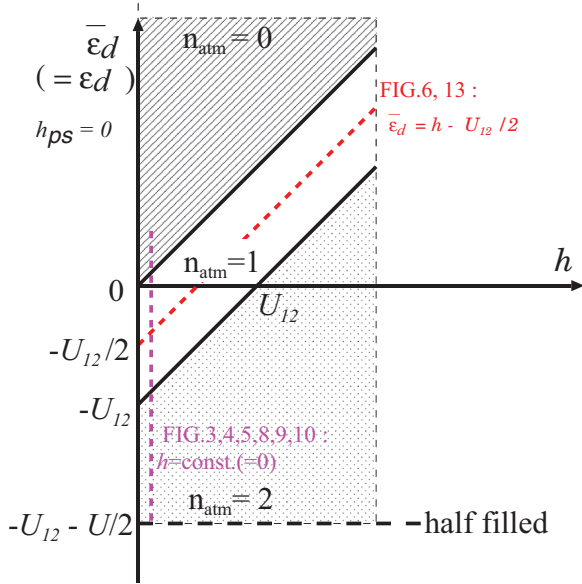


FIG. 2. (Color online) The ground-state electron occupation numbers in the isolated double dot in  $(h, \bar{\epsilon}_d)$  plane at zero pseudospin field  $h_{ps} = 0$ .

#### IV. RESULTS FOR THE RENORMALIZED PARAMETERS

We first of all test the hypothesis that the two-dot model with degenerate levels and a total occupation of the two dots  $n_{d,tot} \sim 1$  has an emergent  $SU(4)$  low-energy fixed point in a regime where fluctuations in the total charge on the two dots are suppressed,  $U/\pi\Gamma \gg 1$  and  $U_{12}/\pi\Gamma \gg 1$ . We first analyze the situation where the on-site energy  $\epsilon_d$  is varied. This corresponds to the line along  $h = 0$  in Fig. 2, which can serve as a guideline.

We consider the cases with parameters similar to those quoted in experiment.<sup>21</sup> Many of the following results are for  $U/\pi\Gamma = 20$ ,  $U_{12}/\pi\Gamma = 5$ , and we take  $\pi\Gamma = 0.01$  in all of the calculations presented here. We consider the case first of all with  $\epsilon_{d,1} = \epsilon_{d,2} = \epsilon_d$  ( $h_{ps} = 0$ ). In Fig. 3(a) we plot  $n_{d,i} = n_d$ , the occupation number on each dot, and the combinations of renormalized parameters  $\tilde{U}\tilde{\rho}(0)$ ,  $\tilde{U}_{12}\tilde{\rho}(0)$ , and  $\tilde{\epsilon}_d/\tilde{\Gamma}$  as a function of the level position on the dots  $\epsilon_d/\pi\Gamma$ .

Over this range the total occupation of the two dots varies from a regime with  $n_{d,tot} \sim 2$ , where  $\tilde{\epsilon}_d/\tilde{\Gamma} \rightarrow 0$ ,  $\tilde{U}\tilde{\rho}(0) \rightarrow 1$ , corresponding to a spin Kondo regime on each dot, to a low-density weakly correlated regime  $n_{d,tot} \sim 0$ , where both  $\tilde{U}\tilde{\rho}(0) \rightarrow 0$  and  $\tilde{U}_{12}\tilde{\rho}(0) \rightarrow 0$ . For  $\epsilon_d/\pi\Gamma \sim -2.5$ , which corresponds to  $\epsilon_d \sim -U_{12}/2$ , there is a region where  $n_{d,tot} \sim 1$  and approximate degeneracy of the spin and interdot excitations.

To check some of the predicted relations between the renormalized parameters we plot the combination  $\tilde{\rho}(0)(\tilde{U} + 2\tilde{U}_{12})$ , relevant for the charge susceptibility in Eq. (11), and the ratios  $\tilde{\epsilon}_d/\tilde{\Gamma}$  and  $\tilde{U}_{12}/\tilde{U}$  in Fig. 3(b). The total occupation of the two dots  $n_{d,tot}$  is also shown.

For  $\epsilon_d/\pi\Gamma < -2.0$  it can be seen that the combination  $\tilde{\rho}(0)(\tilde{U} + 2\tilde{U}_{12})$  is very close to the value of 1, which from Eq. (14) implies a localized regime where the total charge susceptibility of the two dots is negligible, and the fluctuations in the total charge have been almost completely suppressed. This

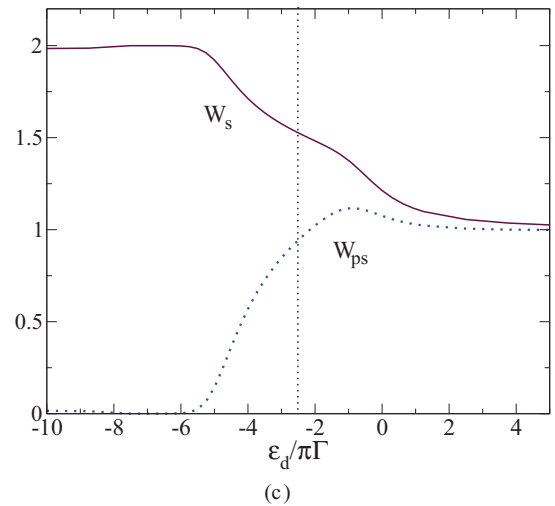
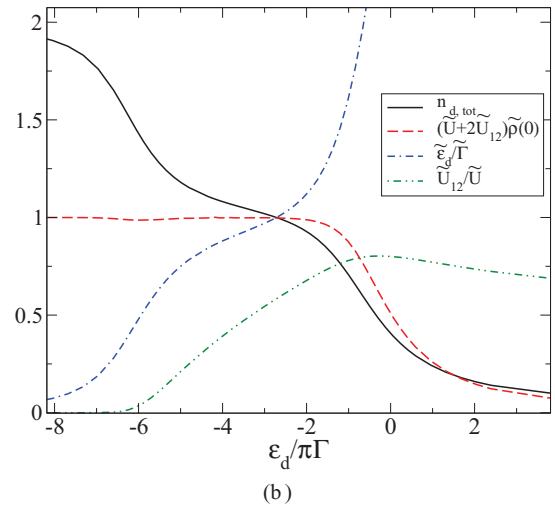
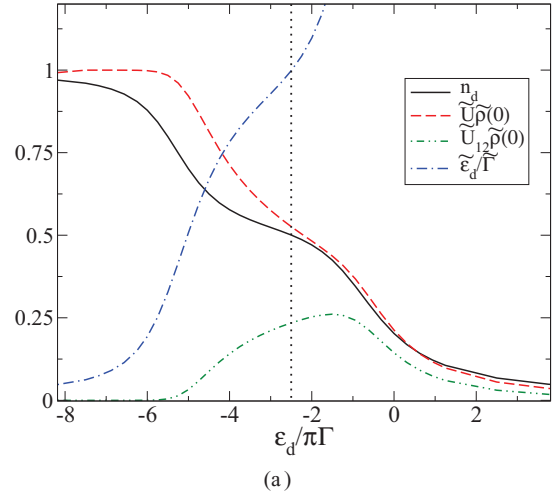


FIG. 3. (Color online) (a) A plot of the occupation number on a single dot  $n_d$ ,  $\tilde{U}\tilde{\rho}(0)$ ,  $\tilde{U}_{12}\tilde{\rho}(0)$ , and  $\tilde{\epsilon}_d/\tilde{\Gamma}$  as a function of  $\epsilon_d/\pi\Gamma$ . (b) A plot of the total occupation number on the dots  $n_{d,tot}$ ,  $\tilde{\rho}(0)(\tilde{U} + 2\tilde{U}_{12})$ ,  $\tilde{\epsilon}_d/\tilde{\Gamma}$ , and  $\tilde{U}_{12}/\tilde{U}$  as a function of  $\epsilon_d/\pi\Gamma$  for the same parameter set. (c) A plot of the Wilson ratios for the spin excitations  $W_s$  and pseudospin excitations  $W_{ps}$  for the double dot as a function of  $\epsilon_d/\pi\Gamma$ . The parameters for all plots are  $U/\pi\Gamma = 20$ ,  $U_{12}/\pi\Gamma = 5$ , and  $\pi\Gamma = 0.01$ . The vertical dotted lines correspond to  $\epsilon_d = -U_{12}/2$ .

regime includes the point of complete degeneracy between the spin and interdot charge fluctuations, where  $\tilde{\varepsilon}_d/\tilde{\Gamma} = 1$  and  $n_{d,\text{tot}} = 1$ , so that all three curves have a common point of intersection, as can be seen clearly in Fig. 3(b). This point to a good approximation corresponds to  $\varepsilon_d = -U_{12}/2$ .

If this degeneracy point corresponded to an SU(4) symmetry for the low-energy excitations then we would expect the ratio  $\tilde{U}_{12}/\tilde{U}$  to pass through this same point giving  $\tilde{U}_{12} = \tilde{U}$ . However, it is of the order 0.45, substantially smaller than 1. The ratio is closer to 1 than that of the bare values  $U_{12}/U = 0.25$ , and hence there is a flow towards the symmetry point, which is however not reached for experimentally relevant parameters. The values  $\tilde{\rho}(0)\tilde{U}_{12} = 0.23$  and  $\tilde{\rho}(0)\tilde{U} = 0.54$  at the degeneracy point give a Wilson ratio  $W_s$  for the spin  $W_s = 1 + \tilde{U}\tilde{\rho}(0) = 1.54$ , and for the pseudospins  $W_{\text{ps}} = 1 + 2\tilde{U}_{12}\tilde{\rho}(0) - \tilde{U}\tilde{\rho}(0) = 0.93$ . As these differ we do not have SU(4) symmetry at the degeneracy point for this parameter set; SU(4) symmetry would require  $W_s = W_{\text{ps}} = 4/3$ .

How the two Wilson ratios,  $W_s$  and  $W_{\text{ps}}$ , vary with  $\varepsilon_d$  for the same parameter set is shown in Fig. 3(c). When  $-U/2 < \varepsilon_d < -U_{12}$ , the interdot interaction  $U_{12}$  plays no significant role and  $\tilde{U}_{12} \rightarrow 0$ . In this regime  $\tilde{U}\tilde{\rho}(0) \rightarrow 1$  which has the effect of suppressing the pseudospin fluctuations so  $W_{\text{ps}} \rightarrow 0$  [see Eq. (20)] and at the same time enhancing the spin Wilson ratio  $W_s \rightarrow 2$ . This corresponds to the spin Kondo limit with a single electron on each dot. As  $\varepsilon_d$  is increased from  $\varepsilon_d = -U_{12}/2$  the value of  $\tilde{U}_{12}$  increases and  $\tilde{U}$  decreases, which has the effect of enhancing  $W_{\text{ps}}$  and reducing  $W_s$ , but as long as the bare interactions obey  $U > U_{12}$ ,  $W_{\text{ps}} < W_s$ . As the level  $\varepsilon_d$  on the dots passes above the Fermi level the interaction terms play very little role and both  $W_{\text{ps}}$  and  $W_s$  asymptotically approach the value 1 corresponding to noninteracting quasiparticles.

For a different parameter set,  $U/\pi\Gamma = 12$ ,  $U_{12}/\pi\Gamma = 6$ , we see that the results are very similar to those presented in Fig. 3(a) but with a slightly increased value of  $\tilde{\rho}(0)\tilde{U}_{12}$  due to the relatively larger value of  $U_{12}$  compared with  $U$ . However, for the parameter set  $U/\pi\Gamma = 12$ ,  $U_{12}/\pi\Gamma = 3$ , with a relatively smaller value of  $U_{12}$  there are some qualitative differences. This is shown in Fig. 4, which

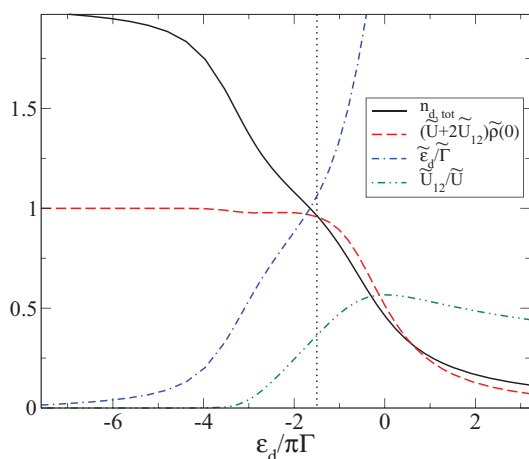


FIG. 4. (Color online) A plot of the total occupation number on the dots  $n_{d,\text{tot}}$ ,  $\tilde{\rho}(0)(\tilde{U} + 2\tilde{U}_{12})$ ,  $\tilde{\varepsilon}_d/\tilde{\Gamma}$ , and  $\tilde{U}_{12}/\tilde{U}$  as a function of  $\varepsilon_d/\pi\Gamma$  for  $U/\pi\Gamma = 12$ ,  $U_{12}/\pi\Gamma = 3$ , where  $\pi\Gamma = 0.01$ . The vertical dotted line corresponds to  $\varepsilon_d = -U_{12}/2$ .

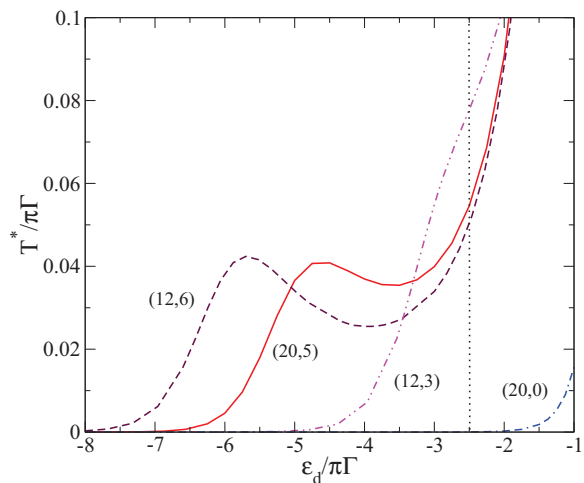


FIG. 5. (Color online) A plot of  $T^*/\pi\Gamma$  as a function of  $\varepsilon_d/\pi\Gamma$  for different parameter sets labeled by the values  $(U/\pi\Gamma, U_{12}/\pi\Gamma)$ . The vertical dotted line corresponds to  $\varepsilon_d = -U_{12}/2$  for case (20,5).

can be compared directly with the corresponding plot in Fig. 3(b).

It can be seen that, due to the smaller value of  $U_{12}/\Gamma$ , the fluctuations of the total charge on the two dots are not suppressed completely so that the value of  $\tilde{\rho}(0)(\tilde{U} + 2\tilde{U}_{12})$  is slightly less than 1 at the spin-pseudospin degeneracy point so that it falls below this point.

As in Eq. (21) we can define an energy scale  $T^*$  via  $4T^* = 1/\tilde{\rho}(0)$ . It has the property  $T^* \rightarrow T_K$ , where  $T_K$  is the spin Kondo temperature in the range where  $n_{d,i} \sim 1$ , defined such that  $\chi_s = 1/4T_K$  for a single dot. A more significant difference between the results for different parameter sets can be seen in Fig. 5 where we plot  $T^*/\pi\Gamma$  as a function of  $\varepsilon_d/\pi\Gamma$ .

For the parameter set  $(U/\pi\Gamma, U_{12}/\pi\Gamma) = (20,5)$  given in Fig. 3 we see that  $T^*$  has a local minimum at  $\varepsilon_d/\pi\Gamma \sim -3.4$  with  $T^*/\pi\Gamma \sim 0.035$ . There is an even more extended and marked minimum for the parameter set (12,6) shown as the dashed curve in Fig. 5. These two results are in marked contrast to the result for  $T^*/\pi\Gamma$  for the case (12,3) with the smaller value of  $U_{12}/\pi\Gamma$  (see Fig. 4), which has no minimum or even a plateau region.

The occurrence of such local minima in  $T^*$  can be accounted for by considering the effective model that results from a Schrieffer-Wolff transformation on the Hamiltonian Eq. (1) (see the Appendix B). For  $0 > \varepsilon_d > -U_{12}$  and  $U \rightarrow \infty$ , fluctuations between the fourfold-degenerate atomic ground states with  $n_d = 1$  are mediated by both the excited two-particle and unoccupied states, so that the resulting effective model features a “pseudospin” exchange coupling  $J_{\text{ps}} \sim -V^2 U_{12}/[\varepsilon_d(\varepsilon_d + U_{12})]$ , which is minimized at the degeneracy point when  $\varepsilon_d = -U_{12}/2$ . This local minimum in  $J_{\text{ps}}$  is sufficient to explain the local minimum in the nominal pseudospin “Kondo temperature,”  $T_{\text{ps}} \sim T^* \sim e^{-1/2\rho_c J_{\text{ps}}}$ , seen in Fig. 5 for the parameter sets with  $U_{12}/\pi\Gamma = 6$  and  $U_{12}/\pi\Gamma = 12$ . Although the two pseudospin projections suggest a correspondence in this regime with an SU(2) pseudospin Kondo model, the spin degrees of freedom modify both the pseudospin Kondo temperature  $T_{\text{ps}}$  from its SU(2) value and the location of the minima in  $T^*$ . The shift of the minimum to the left can be

understood qualitatively by the fact that for large  $U$  the spin Kondo coupling  $J_s \sim -V^2/\varepsilon_d$  is decreasing on decreasing  $\varepsilon_d$ . Hence, due to the interplay of spin and pseudospin Kondo effects the minimum shifts to smaller values of  $\varepsilon_d$ . Specifically, the minimum for the parameter set (20,5) does not correspond to the spin/pseudospin degeneracy point, which occurs where  $\varepsilon_d/\pi\Gamma \sim -2.5$ , giving a value  $T^*/\pi\Gamma \sim 0.055$ . The value of  $T^*$  in this regime is very much greater than the values of  $T_K$  in the spin Kondo regime,  $\varepsilon_d/\pi\Gamma < -8.0$ , which is also shown in Fig. 5 for (20,0). Similar observations were made in Ref. 6, where parameters with  $U_{12}$  closer to  $U$  were studied.

We can make a comparison of  $T^*$  at the degeneracy point with  $T_K$  for an SU(4) model with  $U = U_{12}$  and  $U_{12}/\pi\Gamma = 5.0$ .<sup>32</sup> There are two such SU(4) Kondo models corresponding to the total occupation numbers,  $n_{d,\text{tot}} = 1$  and  $n_{d,\text{tot}} = 2$ . For the SU(4) model with  $n_{d,\text{tot}} = 1$  we find  $T^*/\pi\Gamma = T_K/\pi\Gamma = 0.096$ , which is greater than but of the same order of magnitude as the value  $T^*/\pi\Gamma \sim 0.055$  deduced from the results in Fig. 5 at the degeneracy point. The particle-hole symmetric SU(4) model with  $n_{d,\text{tot}} = 2$  has a somewhat lower value of  $T^*/\pi\Gamma = T_K/\pi\Gamma = 0.031$ .

We can estimate the degree of quasiparticle renormalization at the spin/pseudospin degeneracy point for the parameter set,  $U/\pi\Gamma = 20$ ,  $U_{12}/\pi\Gamma = 5$ , by comparing the value  $T^*$  with that for the noninteracting system where  $n_{d,\text{tot}} = 1$ . At this point,  $\varepsilon_d/\Gamma = 1$  ( $n_{d,\text{tot}} = 1$ ) which gives  $T^*/\pi\Gamma \sim 0.5$ . The degree of renormalization due to the interactions can be estimated from their ratio  $0.5/0.055$ , which gives a renormalization factor of the order of 9 in this case.

In Appendix C we consider a more comprehensive parameter range to test the possibility of an emergent SU(4) low-energy fixed point. In particular we consider the range with very large values of  $U$  and  $U_{12}$ , greater than the conduction band width  $D$ , and we show compatibility of the results with the predictions of a Schrieffer-Wolff transformation which maps onto an SU(4) model in this limit.<sup>6,33,34</sup>

## V. RESULTS IN A FIELD

### A. Crossover as a function of magnetic field $h$

At the degeneracy point where the occupation number on each dot  $n_{d,i} = 0.5$  and  $U \gg \pi\Gamma$  and  $U_{12} \gg \pi\Gamma$ , we have both spin and pseudospin fluctuations. Applying a magnetic field at this point will suppress the spin fluctuations. With a large enough magnetic field it should be possible to suppress the spin fluctuations completely such that there is a crossover to an SU(2) Kondo fixed point due to the pseudospin fluctuations. If this proves to be possible experimentally then one could examine the transport of the two types of pseudospins independently as each is associated with a single dot only. The question naturally arises therefore as to how large the magnetic field has to be to see this crossover. To answer this question we have calculated the renormalized parameters in a magnetic field<sup>28,35</sup> and used them to deduce the Wilson ratios for the spin and pseudospin,  $W_s$  and  $W_{\text{ps}}$ . One way of applying the magnetic field is to adjust the mean level on the dots  $\bar{\varepsilon}_d$  such that  $\bar{\varepsilon}_d = h - U_{12}/2$ , which, starting at  $\varepsilon_d = -U_{12}/2$ , will be such as to maintain the total occupation of the two dots  $n_{d,\text{tot}} = 1$ . This corresponds to the diagonal

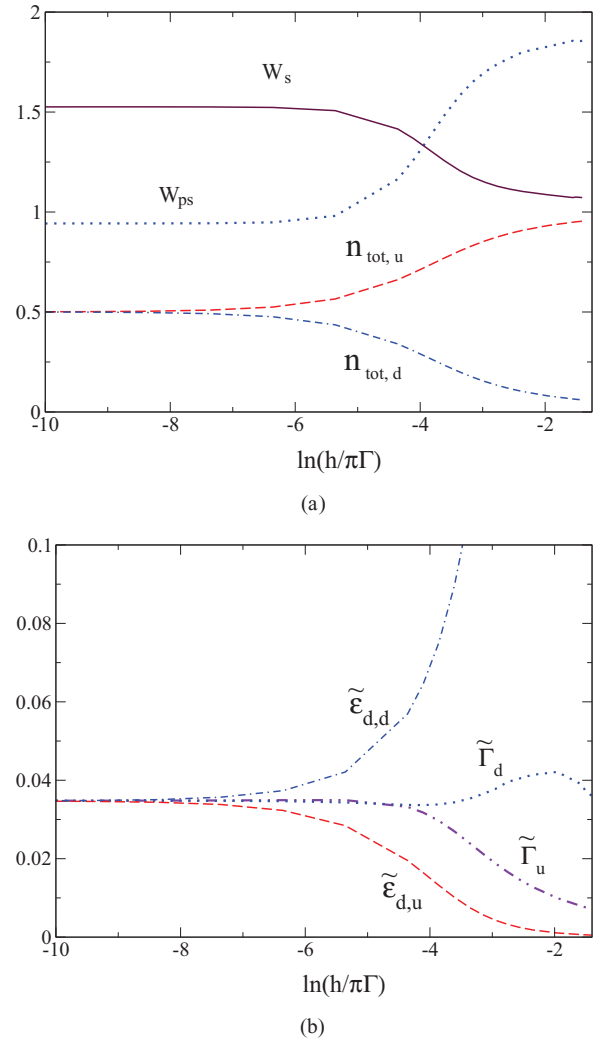


FIG. 6. (Color online) (a) A plot of the Wilson ratios for the spin and pseudospin degrees of freedom,  $W_s$  and  $W_{\text{ps}}$ , and the total spin-up and spin-down occupation numbers  $n_{d,\text{tot},u}$  as a function of  $\ln(h/\pi\Gamma)$  and  $n_{d,\text{tot},d}$ , for the double dot in a magnetic field  $h$ , with a constraint such that  $n_{d,\text{tot}} = 1$  for  $U/\pi\Gamma = 20$ ,  $U_{12}/\pi\Gamma = 5$ ,  $\pi\Gamma = 0.01$ . (b) The corresponding renormalized parameters,  $\tilde{\varepsilon}_{d,x}$  and  $\tilde{\Gamma}_x$ , for the spin-up  $x = u$  and spin-down  $x = d$  quasiparticles in units of  $\pi\Gamma$ .

dashed line in Fig. 2. The results for this case are shown in Fig. 6(a) plotted as a function of  $\ln(h/\pi\Gamma)$  for  $U/\pi\Gamma = 20$ ,  $U_{12}/\pi\Gamma = 5$ ,  $\pi\Gamma = 0.01$ . We have defined  $n_{d,\text{tot},u} = \sum_i n_{d,i,\uparrow}$  and  $n_{d,\text{tot},d} = \sum_i n_{d,i,\downarrow}$ .

For this parameter set we have  $T^*/\pi\Gamma \sim 0.055$  at the degeneracy point corresponding to  $\ln(T^*/\pi\Gamma) \sim -2.9$ . From Fig. 6(a) we can see that the crossover occurs relatively slowly as the magnetic field is increased but when  $h = T^*$ , the pseudospin ratio has risen to a value  $W_{\text{ps}} \sim 1.7$  and the spin ratio fallen to  $W_s \sim 1.14$ . At this point the crossover is well advanced, and so  $T^*$  at the degeneracy point sets the scale of the crossover with the magnetic field  $h$ . However, one needs larger fields to suppress the spin fluctuations fully such that spin ratio  $W_s$  falls to the value 1 and the pseudospin ratio  $W_{\text{ps}}$  reaches the SU(2) Kondo value of 2. From Fig. 6(a), we can extract a rough estimate for the polarizing field  $\ln(h_{\text{pol}}/\pi\Gamma) = -1$ ,  $h_{\text{pol}} \approx 1.16\Gamma$ . Assuming  $\Gamma = 0.01$  meV and  $h = g\mu_B H/2$

with  $|g| = 0.44$  for GaAs,<sup>22</sup> the corresponding magnetic field is  $H = 0.86$  T, well within experimental reach.

In Fig. 6(b) we give the values of the corresponding renormalized parameters  $\tilde{\varepsilon}_d$  and  $\tilde{\Gamma}$  for the up and down quasiparticles. These describe the local spectral function at low energy, where  $\rho_{i,\sigma}(\omega) = z_{i,\sigma} \tilde{\rho}_{i,\sigma}(\omega)$ , with the quasiparticle spectral function from Eq. (8). For  $h = 0$  the quasiparticle resonances for both types of spin lie above the Fermi level at the degeneracy point such that  $\tilde{\varepsilon}_d = \tilde{\Gamma}$ . As the magnetic field is increased the position of the resonance corresponding to the up electrons moves to the Fermi level and narrows considerably. The resonance for the down spin quasiparticle, on the other hand, moves farther away from the Fermi level and initially broadens at the same time but appears to narrow in the very large field regime.

A similar crossover behavior is found if the magnetic field is applied at the degeneracy point without any other adjustment. There is no constraint to maintain  $n_{d,\text{tot}} = 1$ , so in this case there is a second crossover when  $\ln(h/\pi\Gamma) \sim 1$ ,  $h/\pi\Gamma \sim 2.7$ , which occurs when  $h \sim U_{12}/2$ . When  $h > U_{12}/2$  the interdot interaction no longer plays a significant role in determining the occupation numbers on the two dots and the two dots become fully polarized such that  $n_{1,\uparrow} = n_{2,\uparrow} \sim 1$  and  $n_{1,\downarrow} = n_{2,\downarrow} \sim 0$ . Both the spin and pseudospin Kondo effects are suppressed and the Wilson ratios for both spin and pseudospin fall to the value 1.

### B. Crossover as a function of pseudospin field $h_{\text{ps}}$

A similar crossover can occur if we change the relative levels on the two dots so as to induce an effective field  $h_{\text{ps}}$  on the pseudospin degrees of freedom. The results are shown in Fig. 7(a) for the Wilson ratio on dot 1,  $W_{s1}$ , and the pseudospin ratio  $W_{\text{ps}}$ , together with the occupation numbers on the individual dots for the same parameter set with  $\tilde{\varepsilon}_d = -U_{12}/2$ .

The pseudospin field has the effect of suppressing the pseudospin degrees of freedom leaving the spin degrees of freedom on the dots. The spin degrees of freedom, however, depend on the occupation numbers on the individual dots which also change. When  $h_{\text{ps}} > T^*$  the pseudospin degrees of freedom are rapidly suppressed  $W_{\text{ps}} \rightarrow 0$  and the Wilson ratio for the spin on dot 1 has a plateau region with  $W_{s1} \sim 2$ . When  $h_{\text{ps}}$  reaches a value of the order of  $U/2$  [ $\ln(U/2\Gamma) = \ln(10) \sim 2.3$ ] the occupation number on dot 1 rapidly jumps from the order of 1 to 2. As both spin states are then occupied on dot 1 the Wilson ratio  $W_{s1}$  falls to the value 1.

The corresponding renormalized parameters,  $\tilde{\varepsilon}_{d,1}$ ,  $\tilde{\varepsilon}_{d,2}$ ,  $\tilde{\Gamma}_1$ , and  $\tilde{\Gamma}_2$  are shown in Fig. 7(b). In the crossover to the SU(2) spin Kondo regime the peak of the quasiparticle resonance on dot 1 moves to the Fermi level while the quasiparticle resonance on dot 2 moves above the Fermi level in a very similar way to that for the up and down electrons shown in Fig. 6(b). The values of  $\tilde{\varepsilon}_{d,1}$  and  $\tilde{\varepsilon}_{d,2}$  are almost identical with  $\tilde{\varepsilon}_{d,u}$  and  $\tilde{\varepsilon}_{d,d}$  for  $h = h_{\text{ps}}$ . There is a distinct difference, however, in the values of the corresponding widths. In the pseudofield  $h_{\text{ps}}$  the quasiparticle resonance that moves to the Fermi level narrows much more rapidly than the corresponding one in a magnetic field  $h$ , while the one that moves away from the Fermi level broadens more markedly and monotonically. The narrower

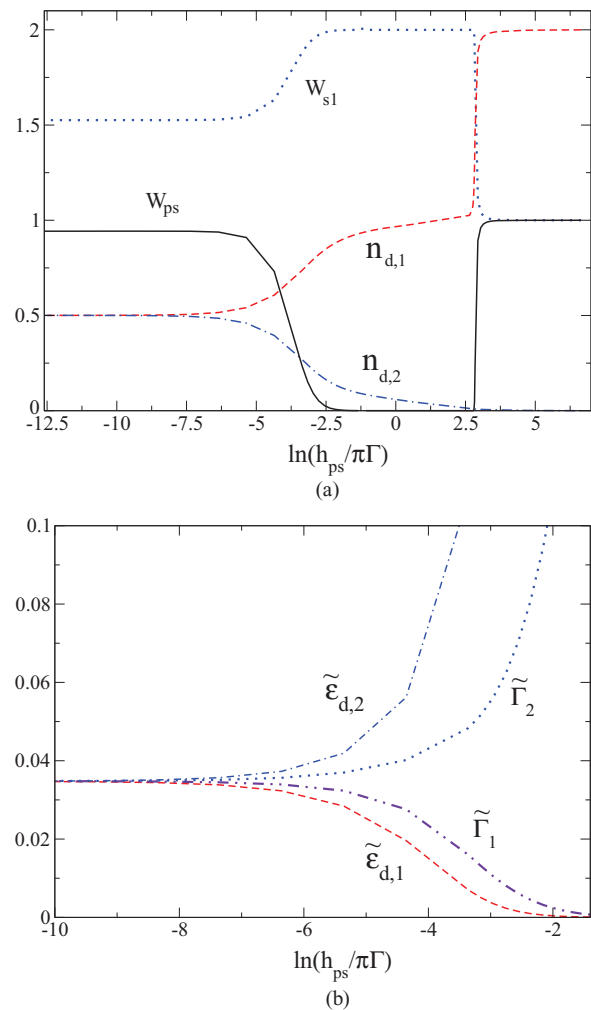


FIG. 7. (Color online) (a) A plot of the spin Wilson ratio  $W_{s1}$  on dot 1, the pseudospin ratio  $W_{\text{ps}}$ , and the occupation numbers for the two dots,  $n_{d,1}$  and  $n_{d,2}$ , as a function of  $\ln(h_{\text{ps}}/\pi\Gamma)$  for  $U/\pi\Gamma = 20$ ,  $U_{12}/\pi\Gamma = 5$ ,  $\tilde{\varepsilon}_d = -U_{12}/2$ ,  $\pi\Gamma = 0.01$ . (b) A corresponding plot of the renormalized parameters  $\tilde{\varepsilon}_{d,1}$ ,  $\tilde{\varepsilon}_{d,2}$ ,  $\tilde{\Gamma}_1$ , and  $\tilde{\Gamma}_2$  in units of  $\pi\Gamma$  (note the smaller range).

resonance at the Fermi level in the pseudospin case is due to the much smaller value of  $T_K$  in the SU(2) spin Kondo limit, when the pseudospin excitations are fully suppressed, compared with the SU(2) pseudospin Kondo limit, when the spin fluctuations are suppressed.

Similar shifts in the spectral density are found in a study of a crossover from an SU(4) to an SU(2) Kondo state by Tosi *et al.* in Ref. 36 using the noncrossing approximation (NCA) at finite temperature. However in their case the level on one dot only was increased, whereas in our calculation the levels were changed to keep the average of the levels on the two dots constant to mimic the magnetic field case; however, qualitatively the results are similar. In the NCA calculation the lower atomic peak is seen in addition to the quasiparticle resonance on the approach to the spin SU(2) Kondo regime. This atomic peak is absent in  $\tilde{\rho}_{i,\sigma}(\omega)$  which only describes the low-energy quasiparticle excitations.

## VI. DIFFERENTIAL CONDUCTANCE

A quantity well accessible in experiment is the differential conductance. The current through dot  $i$ ,  $I_i$ , is given by the result of Meir and Wingreen,<sup>37</sup>

$$I_i = \frac{2e\bar{g}_i}{\pi\hbar} \sum_{\sigma} \int_{-\infty}^{\infty} d\omega [f_s(\omega) - f_d(\omega)] [-\text{Im}G_{d,i,\sigma}^r(\omega, V_{ds,i})], \quad (22)$$

where  $\bar{g}_i = \Gamma_{d,i}\Gamma_{s,i}/(\Gamma_{d,i} + \Gamma_{s,i})$ ,  $G_{d,i,\sigma}^r(\omega, V_{ds,i})$  is the steady-state retarded Green's function on the dot site, and  $f_s(\omega)$ ,  $f_d(\omega)$  are Fermi distribution functions for the electrons in the source and drain reservoirs, respectively,  $f_{\alpha}(\omega) = f_F(\omega - \mu_{\alpha})$  and  $\mu_{s,i} = \alpha_{s,i}eV_i$ ,  $\mu_{d,i} = -\alpha_{d,i}eV_i$ , so that for a difference in chemical potential across dot  $i$  of  $eV_i$  due to the bias voltage,  $V_i$ ,  $\alpha_{s,i} + \alpha_{d,i} = 1$ .

### A. Results at $T = 0$

In the limit of zero temperature and in the absence of a magnetic field, the zero bias differential conductance through dot  $i$ ,  $G_i = dI_i/dV$ , reads,

$$G_i = 4\pi\bar{g}_i\rho_i(0)G_0, \quad (23)$$

where  $G_0 = 2e^2/h$  is the twice the quantum conductance result. This can be expressed in terms of renormalized parameters, via  $\rho_i(0) = z_i\tilde{\rho}_i(0)$ ,

$$G_i = \frac{g_i G_0}{1 + \left(\frac{\tilde{\varepsilon}_{d,i}}{\tilde{\Gamma}_i}\right)^2}, \quad (24)$$

where  $g_i = 4\bar{g}_i/(\Gamma_{d,i} + \Gamma_{s,i})$ . In the spin Kondo regime,  $\tilde{\varepsilon}_{d,i}/\tilde{\Gamma}_i \rightarrow 0$  such that  $G_i \rightarrow g_i G_0$ , which is the unitary limit for symmetric coupling to the leads,  $\Gamma_{d,i} = \Gamma_{s,i}$  so  $g_i = 1$ . At the degeneracy point we have  $\tilde{\varepsilon}_{d,i}/\tilde{\Gamma}_i = 1$ , such that in this case  $G_i = g_i G_0/2$ . Generally, in most experimental situations one has  $\Gamma_{d,i} \neq \Gamma_{s,i}$ . The crossover of the described behavior can be seen in Fig. 8 where we plot  $G_i/g_i G_0$  as a function

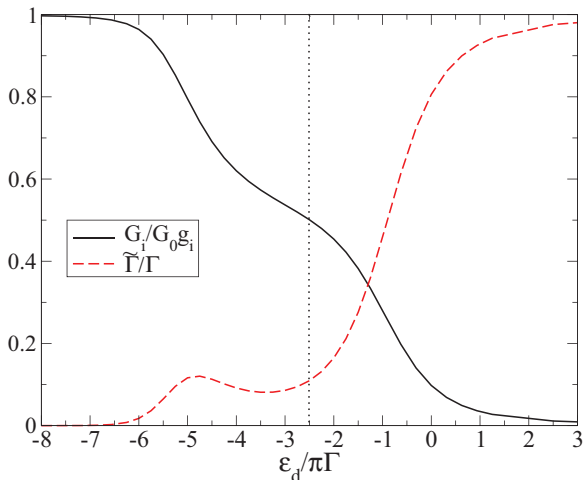


FIG. 8. (Color online) A plot of  $G_i/g_i G_0$  and  $\tilde{\Gamma}/\Gamma$  as a function of  $\varepsilon_d/\pi\Gamma$  for the model with  $U/\pi\Gamma = 20$ ,  $U_{12}/\pi\Gamma = 5$ , and  $\pi\Gamma = 0.01$ . The vertical dotted line corresponds to  $\varepsilon_d = -U_{12}/2$ .

of  $\varepsilon_d/\pi\Gamma$  for the parameters  $U/\pi\Gamma = 20$ ,  $U_{12}/\pi\Gamma = 5$ , and  $\pi\Gamma = 0.01$ .

Also plotted is the ratio  $\tilde{\Gamma}/\Gamma$ , because this gives a measure of the width of the quasiparticle resonance to be seen in the spectral density at zero temperature in terms of that for the noninteracting system  $\Gamma$ . The quasiparticle resonance is seen as a peak in the measurement of the differential conductance versus source drain voltage  $V$ . Our calculations therefore predict a minimum of the width of the source drain signal when the gate voltage is tuned along the ridge with enhanced conductance. The conductance signals in Figs. 2(a) and 2(b) of Ref. 22 seem to indicate the possibility of such a behavior; however, a closer inspection of the experimental data would be desirable. If this resonance is very narrow, as it can be in the spin Kondo regime due to the exponential renormalization due to  $U$ , the peak will not be detectable if the resolution of the temperature of the experiment is such that  $T > \tilde{\Gamma}$ . This is the situation in the experiments reported in Refs. 21 and 22 but the peak in the spin/pseudospin degeneracy regime is seen where the value of  $\tilde{\Gamma}$  is significantly less renormalized than in the spin Kondo regime (see below). The conductance in the presence of a magnetic and pseudospin field and the associated crossovers are discussed in Appendix D.

### B. Results at finite temperature

So far we have dealt with the situation at zero temperature. However, the scale for spin Kondo can be very small such that the finite temperature  $T$  in the experiment matters. A more general expression for the zero bias differential conductance reads

$$G_i(T) = \frac{2e\bar{g}_i}{\hbar} \sum_{\sigma} \int_{-\infty}^{\infty} d\omega \beta e^{\beta\omega} f_F(\omega)^2 \rho_{d,i,\sigma}(\omega), \quad (25)$$

where  $\beta = 1/T$ . We expect that much of the change of the conductance with temperature arises from the change in the renormalization of the quasiparticles on energy scales of the order of the temperature  $T$ , such that we can approximate  $\rho_{d,i,\sigma}(\omega)$  by the  $T = 0$  expression but in terms of temperature-dependent renormalized parameters,

$$\rho_{d,i,\sigma}(\omega) = \frac{1}{\pi\Gamma} \frac{\tilde{\Gamma}_i^2(T)}{[\omega - \tilde{\varepsilon}_{d,i}(T)]^2 + \tilde{\Gamma}_i(T)^2}. \quad (26)$$

The extension to temperature-dependent renormalized parameters was previously used to calculate the temperature dependence of the spin susceptibility for the Anderson model in the Kondo limit and an excellent agreement with the exact results from the Bethe ansatz was obtained.<sup>25,27</sup> The temperature dependence of the renormalized parameters can be estimated from the NRG calculations for an iteration  $N$ . The  $N$ -dependent parameters calculated using Eq. (A4) are converted into ones corresponding to a temperature  $T_N$  given by

$$T_N = \eta D \Lambda^{\frac{1-N}{2}}, \quad (27)$$

where  $D$  is half the conduction electron bandwidth and  $\eta$  is a constant of order 1.<sup>38</sup> The approximation for the temperature dependence of conductance is tested in Appendix E with



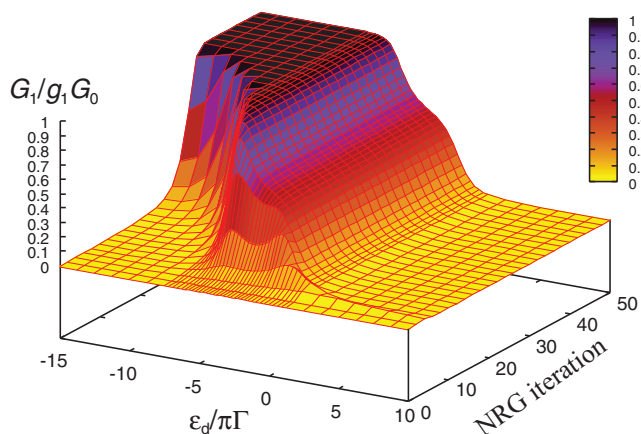


FIG. 9. (Color online) A two-dimensional plot of the linear conductance ratio  $G(T_N)/g_1 G_0$  as a function of  $\varepsilon_d/\pi\Gamma$  and the NRG iteration number  $N$  which corresponds to a temperature  $T_N = 0.55\Lambda^{(1-N)/2}$  with  $\Lambda = 6$  for the parameter set  $U/\pi\Gamma = 20$ ,  $U_{12}/\pi\Gamma = 5$ , and  $\pi\Gamma = 0.01$ .

results of a recent paper by Merker *et al.*,<sup>39</sup> and excellent agreement is found.

In Fig. 9 we give a two-dimensional plot of the linear conductance ratio  $G(T_N)/g_1 G_0$  as a function of  $\varepsilon_d/\pi\Gamma$  using renormalized parameters corresponding to the NRG iteration number  $N$  for the parameter set  $U/\pi\Gamma = 20$ ,  $U_{12}/\pi\Gamma = 5$ .

We estimate the corresponding temperature dependence from the relation in Eq. (27), with  $D = 1$ ,  $\Lambda = 6$ , and  $\eta = 0.55$ . The value of  $\eta$  was selected by the requirement that the calculated entropy  $S_{\text{imp}}(T_N = \eta D \Lambda^{\frac{1-N}{2}}) \rightarrow 0$  for large  $N$ . The effect of increasing temperature (reducing  $N$ ) can be seen to significantly reduce the conductance in the most strongly correlated regime  $\varepsilon_d/\pi\Gamma < -6$  when the temperature exceeds the very small values of the Kondo temperature, and the Kondo resonance in the vicinity of the Fermi level is suppressed. At higher temperatures ( $N \sim 10$ ) a two-peaked response develops as a function of  $\varepsilon_d/\pi\Gamma$ . This can be seen more clearly in Fig. 10, where we extract the

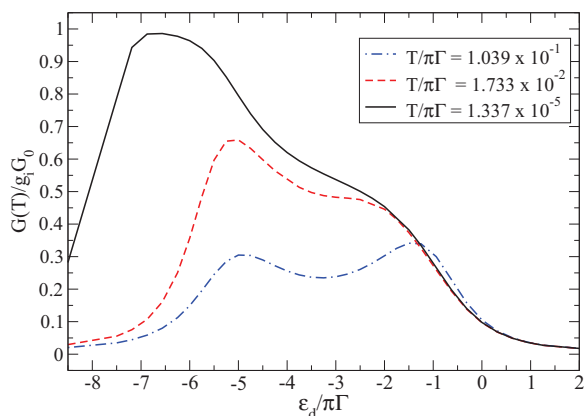


FIG. 10. (Color online) The linear conductance  $G(T)/g_1 G_0$  as a function of  $\varepsilon_d/\pi\Gamma$  taken from the results in Fig. 9 for  $T/\pi\Gamma = 0.104, 0.0173, 1.34 \times 10^{-5}$  corresponding to  $N = 8, 10, 18$ .

results for  $T/\pi\Gamma = 0.104, 0.0173, 1.34 \times 10^{-5}$ , which span the interesting temperature regime.

For this parameter set we have estimated  $T^*/\pi\Gamma = 0.055$  at the spin/pseudospin degeneracy point, so for  $T \sim T^*$  this falls within the two-peak regime. As the temperature is increased in the temperature range  $T \sim T^*$ , the heights of both peaks are reduced but the height of the peak at the larger value of  $|\varepsilon_d|$  decreases more rapidly. As a consequence the two-peak structure becomes more symmetrical. At the higher temperature  $T/\pi\Gamma = 0.1039$ , where  $T \sim 2T^*$ , the height of the peak corresponding to the lower value of  $|\varepsilon_d|$  begins to become the larger of the two. We have calculated further results for the conductance as a function of  $N$  or  $T$  corresponding to Figs. 9 and 10 for  $U/\pi\Gamma = 20$  with  $U_{12}/\pi\Gamma = 10, 15, 20$ , and find the same features persist as in those shown for  $U_{12}/\pi\Gamma = 5$ .

Though we have not used the particular parameter set for the recently reported experimental results by Keller *et al.*,<sup>22</sup> we find a two-peak form and general trend with temperature as shown in Fig. 2 of their paper (note that the results there are plotted as a function of  $-\varepsilon_d$ ). In Fig. 10 it can be seen that there is a range  $0 > \varepsilon_d/\pi\Gamma > -1$  where the conductance increases with temperature rather than decreases. The behavior is similar in the results shown in Fig. 2(d) of Ref. 22. We conclude that the quasiparticle picture with temperature-dependent parameters can provide an explanation of the main features seen in the experimental results.

In Fig. 3 of Ref. 22 also the temperature scaling is analyzed and NRG calculations for experimental parameters show a small bump around 30 mK. The peak of the spectral function in this regime is at  $\tilde{\varepsilon}_d$ , shifted from the Fermi level  $\omega = 0$ . Therefore, as also seen in Fig. 15 it is possible that the conductance increases at finite temperature since additional spectral weight can become available for transport. A similar effect was observed when the Kondo resonance splits in a magnetic field.<sup>28</sup> It is possible that such an effect is responsible for the experimental observation in Ref. 22. These features, however, are likely to depend on the particular parameter set used in the calculations.

## VII. CONCLUSIONS

We have surveyed the low-energy behavior for a double quantum dot system described by an Anderson model paying particular attention to the parameter regime where the spin and pseudospin (interdot) excitations become degenerate. In an earlier theoretical study it has been asserted that the strong correlation behavior in this regime would correspond to that of an SU(4) Kondo model.<sup>3</sup> To examine this assertion we have calculated the parameters that specify the effective Hamiltonian for the low-energy regime, which correspond to renormalized versions of the parameters,  $\varepsilon_{d,i}$ ,  $\Gamma_i$ ,  $U_i$ , and  $U_{12}$ , which describe the original “bare” model. They can be accurately deduced from an analysis of the low-energy excitations of an NRG calculation.<sup>25,26</sup> The low-energy effective model describes a Fermi liquid in which the quasiparticles interact via the terms  $\tilde{U}$  and  $\tilde{U}_{12}$ . There is a point of 4-fold degeneracy for the effective Hamiltonian when the interaction terms between the quasiparticles set to zero,  $\tilde{U} = \tilde{U}_{12} = 0$ . For universality and an SU(4) fixed point, however, we require that

the low-energy response functions can be expressed in terms of a *single* renormalized energy scale, the Kondo temperature  $T_K$ . Once the interaction terms are included the SU(4) symmetry survives only if  $\tilde{U} = \tilde{U}_{12}$ . For  $U \leq D$  we find this to be the case only if  $U = U_{12}$  so no new symmetry emerges on the low-energy scale. This implies that for  $U > U_{12}$  and  $U \leq D$  we require two renormalized parameters to specify the low-energy behavior. For  $U \gg D$  and  $U_{12} > D$  (see Appendix C), there is a regime where we do find SU(4) symmetry. This is consistent with the derivation of an SU(4) Coqblin-Schrieffer model based on a Schrieffer-Wolff transformation.<sup>6,33,34</sup> This regime is not expected to be one relevant to the experimental situation as the cutoff on the bath density of states  $D$  is expected to be greater than the interlevel spacing on the dots.

The question arises as to why the conclusions based on the Schrieffer-Wolff (SW) transformation apply in the single-impurity case for  $U < D$ , but do not apply here. In the single Anderson impurity case with  $U/\pi\Gamma \gg 1$  the SW mapping to the SU(2) Kondo model holds strictly only when the energy levels of the impurity,  $\varepsilon_d$  and  $\varepsilon_d + U$ , lie outside the conduction band. The resulting mapping to the Kondo model however still holds if  $\varepsilon_d$  or  $\varepsilon_d + U$  fall within the band but the prefactor in the expression for the Kondo temperature is modified due to virtual charge scattering via band states  $\varepsilon$  lying in the regime  $|\varepsilon| > |\varepsilon_d|, |\varepsilon_d + U|$ . Here, however, we are not just dealing with spin fluctuations but also pseudospin or charge fluctuations. We can expect the pseudospin terms to be more significantly modified by the virtual charge excitations which can occur in the regime within the band when  $U, U_{12} < D$ .

We note that there is not a unique SU(4) Kondo model for the double quantum dot. The Anderson model with  $U_{12} = U$  can be mapped into a SU(4) Kondo model also in the case with particle-hole symmetry with  $n_{d,1} = n_{d,2} = 1$ .<sup>34</sup> In this case the operators in the model correspond to a 6-dimensional representation of SU(4) in contrast to the mapping for the spin/pseudospin degenerate model with  $n_{d,1} = n_{d,2} = 0.5$  where the operators correspond to the fundamental (4-dimensional) representation of SU(4).

The regime with spin/pseudospin degeneracy has attracted experimental interest<sup>20-22</sup> as it raises the possibility of using the pseudospin excitations, which can be manipulated and observed in independent channels, as a more convenient way to examine behavior of excitations in individual spin species. There are also recent proposals to use double-dot systems for thermoelectric applications<sup>40</sup> and to create spin-polarized currents<sup>41,42</sup> (cf. Fig. 13). Experimental measurements have been made of electron transport through the individual dots subject to bias voltages applied to the separate conduction electron baths and there are recent theoretical predictions for this situation.<sup>36</sup> The results for the conductance as a function of the bias voltage correspond to non-equilibrium steady-state conditions and present a major challenge to theory. The linear response, however, can be deduced from equilibrium calculations. At  $T = 0$  the linear response depends only on the free quasiparticles, and at the degeneracy point the result does correspond to that for an SU(4) model, which via the Friedel sum rule can be expressed in terms of the equilibrium occupation numbers on the dots. Our calculations of the conductance, extended to finite temperatures, based on the

assumption of temperature-dependent but free quasiparticles, predicts features in line with the experimental results. It provides a framework for their interpretation.

The quasiparticle interactions  $\tilde{U}_i, \tilde{U}_{12}$  will play some role in the temperature dependence of the conductance and result in some deviation from universal SU(4) Kondo behavior. There is a contribution to the leading  $T^2$  correction to the conductance in the SU(2) Anderson and Kondo models arising from the quasiparticle interaction term  $\tilde{U}$ . These terms can be calculated exactly in terms of renormalized parameters using the renormalized perturbation expansion (RPT).<sup>28-30</sup> Le Hur *et al.*<sup>19</sup> have predicted that for an SU(4) Kondo model the temperature corrections of order  $T^2$  cancel out in the conductance so the leading contribution in this case is of order  $T^3$ . Away from SU(4) symmetry when  $\tilde{U}_{12} \neq \tilde{U}$ , this cancellation cannot be complete so that a  $T^2$  contribution should remain. This issue is currently being investigated. Calculations can also be carried out for the leading corrections to the linear voltage regime in powers of the bias voltage  $V$ , using RPT in the Keldysh formulation, as have already been carried out for the single-impurity model.<sup>43-45</sup>

## ACKNOWLEDGMENTS

We would like to acknowledge helpful discussions with T. Costi, D. Goldhaber-Gordon, B. Halperin, A. Keller, D. Logan, and G. Zaránd. We thank T. Costi and co-authors for supplying the numerical results on the temperature dependence of conductance for the Anderson model from their paper<sup>39</sup> for inclusion in Fig. 15. J.B. acknowledges financial support from the DFG through BA 4371/1-1. Numerical computation in this work was partially carried out at the Yukawa Institute Computer Facility. This work has been supported in part by EPSRC Mathematics Platform Grant No. EP/1019111/1.

## APPENDIX A: CALCULATION OF THE RENORMALIZED PARAMETERS

In an NRG calculation for a single-impurity Anderson model the conduction electron band is discretized and cast into a form corresponding to a tight-binding chain coupled to the impurity at one end by the hybridization parameter  $V$ .<sup>38,46</sup> The noninteracting single-particle Green's function for dot  $i$  then takes the form

$$G_{d,i,\sigma}^{(0)}(\omega) = \frac{1}{\omega - \varepsilon_d - V^2 G_{0,i,\sigma}^{(0)}(\omega)}, \quad (\text{A1})$$

where

$$G_{n,i,\sigma}^{(0)}(\omega) = \frac{1}{\omega - \varepsilon_i - V_n^2 G_{n+1,i,\sigma}^{(0)}(\omega)}, \quad (\text{A2})$$

with  $n = 0, 1, 2, \dots, N$ , where  $V_n$  are the intersite hopping matrix elements and  $\varepsilon_n$  the energies along the conduction electron chain, with  $V_n = \Lambda^{-n/2} \xi_n$ , where  $\Lambda (> 1)$  is the discretization parameter, and  $\xi_n$  is given by

$$\xi_n = \frac{D}{2} \frac{(1 + \Lambda^{-1})(1 - \Lambda^{-n-1})}{(1 - \Lambda^{-2n-1})^{1/2}(1 - \Lambda^{-2n-3})^{1/2}}. \quad (\text{A3})$$

The poles of the Green's function (A1) give the single-particle excitations for the non-interacting system.

We can identify the low-energy free quasiparticle excitations of the *interacting* system with the poles of this same Green's function but with renormalized parameters  $\tilde{\varepsilon}_d$  and  $\tilde{V}$ . If  $E_{p,\alpha}(N)$  and  $E_{h,\alpha}(N)$  are the lowest energies of single particle and hole excitations calculated for a NRG chain of length  $N$  then we can take these as corresponding to the poles of (A1) with an  $N$ -dependent hybridization  $\tilde{V}(N)$  and energy level  $\tilde{\varepsilon}_d(N)$ . We then get the two equations

$$\pm E_{p/h,i}(N) - \tilde{\varepsilon}_d(N) - \tilde{V}(N)^2 G_{0,i,\sigma}^{(0)}(\pm E_{p/h,i}(N)) = 0 \quad (\text{A4})$$

to deduce  $\tilde{V}(N)$  and energy level  $\tilde{\varepsilon}_d(N)$ . The values of  $\tilde{\varepsilon}_d$  and  $\tilde{V}$  can be identified with the values in the plateau regime for large  $N$ ,  $\tilde{\varepsilon}_d = \lim_{N \rightarrow \infty} \tilde{\varepsilon}_d(N)$  and  $\lim_{N \rightarrow \infty} \tilde{V}(N) = \tilde{V}$ , with  $\tilde{\Gamma} = \pi \tilde{V}^2 / 2D$ .

After diagonalizing the free quasiparticle Hamiltonian, the renormalized interaction parameters,  $\tilde{U}$ ,  $\tilde{J}$ , and  $\tilde{U}_{12}$ , can be calculated from the leading order correction terms to the difference between the lowest two particle excitations,  $E_{pp,i}^\sigma(N)$ , and the two lowest single-particle excitations for large  $N$ , e.g.,  $E_{pp,i}^0(N) - E_{p,i}^\uparrow(N) - E_{p,i}^\downarrow(N)$  in channel  $i$  determines  $\tilde{U}_i$ . Once the renormalized parameters have been determined the  $T = 0$  susceptibilities and specific-heat coefficient  $\gamma$  can then be determined by substituting them into the relevant RPT equations. For further details we refer to earlier papers.<sup>25,26,32,34</sup>

## APPENDIX B: EFFECTIVE HAMILTONIANS

An effective Hamiltonian for the model with  $U \rightarrow \infty$  and  $U_{12} > |\varepsilon_d| \gg \pi\Gamma$  can be found by projecting the full Hamiltonian onto its atomic (i.e.,  $\Gamma = 0$ ) ground states and including the effects of fluctuations between these ground states perturbatively to lowest order in  $\Gamma$ . For  $V_{k,1} = V_{k,2} = V_k$ , the impurity contribution to the resulting effective Hamiltonian is

$$H_{\text{eff}} = \sum_{kk'\sigma\sigma'} [J_{\perp}^{kk'} \{ (l_{\sigma\sigma'}^{kk'})^+ L_{\sigma'\sigma}^- + (l_{\sigma\sigma'}^{kk'})^- L_{\sigma'\sigma}^+ \} + J_{\parallel}^{kk'} (l_{\sigma\sigma'}^{kk'})^z L_{\sigma'\sigma}^z] + \sum_{kk'i} J_{\text{spin}}^{kk'} \mathbf{s}_{kk'i} \cdot \mathbf{S}_i, \quad (\text{B1})$$

where  $S_i^\alpha = \frac{1}{2} c_{d,i,\sigma}^\dagger \sigma_{\sigma\sigma'}^{(\alpha)} c_{d,i,\sigma'}$  and we have introduced the pseudospin raising operator  $L_{\sigma\sigma'}^+ \equiv |1\sigma\rangle\langle 2\sigma'|$  and lowering operator  $L_{\sigma\sigma'}^- \equiv |2\sigma\rangle\langle 1\sigma'|$  and similarly for the conduction electrons, with  $(l_{\sigma\sigma'}^{kk'})^+ = c_{k,1,\sigma}^\dagger c_{k',2,\sigma'}$ , etc., where  $c_{k,i,\sigma} = c_{k,i,s,\sigma} + c_{k,i,d,\sigma}$  (i.e., appropriate to the situation close to equilibrium). Here,  $|i\sigma\rangle$  denotes the impurity configuration with one electron of spin  $\sigma = \uparrow, \downarrow$  on the dot  $i = 1, 2$  and the last term in Eq. (B1) describes a normal Kondo spin exchange occurring independently on dots 1 and 2. The pseudospin contribution is anisotropic, with  $J_{\perp}^{kk'} = -V_k V_{k'}^* U_{12} / \varepsilon_d (\varepsilon_d + U_{12})$  and  $J_{\parallel}^{kk'} = 2V_k V_{k'}^* / (\varepsilon_d + U_{12})$ , whereas the spin contribution is isotropic with an antiferromagnetic exchange coupling  $J_{\text{spin}}^{kk'} = -V_k V_{k'}^* / \varepsilon_d$ . Poor man's scaling equations<sup>3,16,17,47</sup> for this effective model show the mutual influence of spin and pseudospin Kondo physics as visible in the renormalization of the respective couplings.

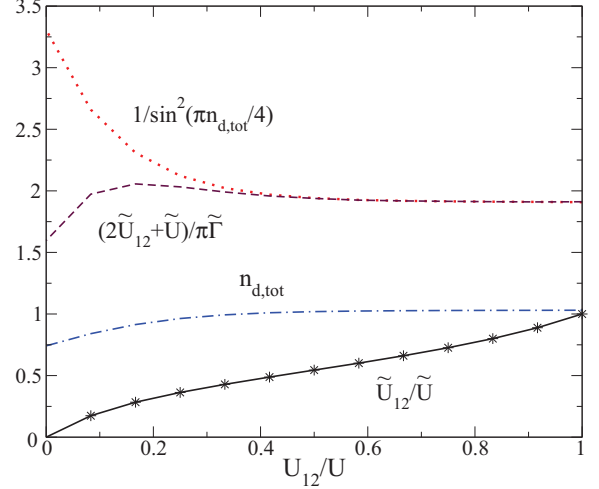


FIG. 11. (Color online) A plot of  $n_{d,\text{tot}}$ ,  $(2\tilde{U}_{12} + \tilde{U})/\pi\tilde{\Gamma}$ ,  $1/\sin^2(\pi n_{d,\text{tot}}/4)$ , and  $\tilde{U}_{12}/\tilde{U}$  as a function of  $U_{12}/U$  for  $\varepsilon_d = -U_{12}/2$ .

## APPENDIX C: RENORMALIZED PARAMETERS FOR AN EXTENDED PARAMETER RANGE

To test more generally the possibility of an emergent SU(4) low-energy fixed point in the regime  $U/\pi\Gamma \gg 1$ ,  $U_{12}/\pi\Gamma \gg 1$  with  $n_{d,\text{tot}} \sim 1$ , we have calculated the renormalized parameters  $\tilde{U}$ ,  $\tilde{U}_{12}$ ,  $\tilde{\Gamma}$ , and  $\tilde{\varepsilon}_d$  as a function of  $U_{12}$  for the case  $U/\pi\Gamma = 12$  with  $\varepsilon_d = -U_{12}/2$ . The condition that the total charge susceptibility of the dots be negligible from Eq. (14) is  $(2\tilde{U}_{12} + \tilde{U})\tilde{\rho}(0) = 1$ . Using the Friedel sum rule Eq. (9), this condition can be alternatively expressed as

$$\frac{(2\tilde{U}_{12} + \tilde{U})}{\pi\tilde{\Gamma}} = \frac{1}{\sin^2(\pi n_{d,\text{tot}}/4)}. \quad (\text{C1})$$

In Fig. 11 we plot the results for  $n_{d,\text{tot}}$ ,  $(2\tilde{U}_{12} + \tilde{U})/\pi\tilde{\Gamma}$ ,  $1/\sin^2(\pi n_{d,\text{tot}}/4)$ , and  $\tilde{U}_{12}/\tilde{U}$ , as a function of  $U_{12}/U$ . The condition in Eq. (C1) holds to a good approximation for the range  $U_{12}/U > 0.4$  and also over this range that the total charge on the dots  $n_{d,\text{tot}} \sim 1$ . The condition for a low-energy SU(4) fixed point  $\tilde{U}_{12}/\tilde{U} = 1$ , however, is only satisfied at the point  $U_{12} = U$ , i.e., only if we have SU(4) symmetry already for the “bare” model. At the SU(4) fixed point using Eq. (C1) we predict

$$\frac{\tilde{U}}{\pi\tilde{\Gamma}} = \frac{\tilde{U}_{12}}{\pi\tilde{\Gamma}} = \frac{1}{3\sin^2(\pi n_{d,\text{tot}}/4)}, \quad (\text{C2})$$

which is satisfied precisely in the results in Fig. 11. For these results with  $\varepsilon_d = -U_{12}/2$  and  $U_{12}/\pi\Gamma \gg 1$ ,  $n_{d,\text{tot}} \sim 1$  but not precisely equal to 1. In an earlier study of the SU(4) version of this model<sup>34</sup> we calculated the renormalized parameters keeping  $n_{d,\text{tot}}$  strictly equal to 1. In that case we obtained the result  $\tilde{U}/\pi\tilde{\Gamma} = 0.66665$  asymptotically for large  $U$  in very accurate agreement with the prediction from Eq. (C2),  $\tilde{U}/\pi\tilde{\Gamma} = 2/3$ .

We get a very similar picture to that shown in Fig. 11 if we take a larger value of  $U$ ,  $U/\pi\Gamma = 20$ ,  $\varepsilon_d = -U_{12}/2$  and vary  $U_{12}$ . We find  $\tilde{U}_{12}/\tilde{U} = 1$  only when  $U_{12} = U$ . For a given ratio  $U_{12}/U$ , the ratio of  $\tilde{U}_{12}/\tilde{U}$  is observed to be larger

in the range  $U_{12} < U$  when we increase the value of  $U$  from  $U/\pi\Gamma = 12$  to  $U/\pi\Gamma = 20$ . The question arises as to whether the ratio  $\tilde{U}_{12}/\tilde{U}$  would approach the value 1 in this range if we increase the value of  $U$  still further. For  $U > 20\pi\Gamma = 0.2D$  ( $D = 1$ ,  $\pi\Gamma = 0.01$ ), the values of  $U$  become of the order of the half bandwidth  $D$ . With  $U \sim D$  and  $\varepsilon_d = -U_{12}/2$  in the range  $U_{12} \rightarrow U$ , the ground-state impurity level will become far removed from the Fermi level resulting in a renormalized energy scale  $T^* \rightarrow 0$ .

To investigate the larger  $U$  regime we take a fixed value for  $\varepsilon_d$ , just below the Fermi level  $\varepsilon_d = -3\pi\Gamma$ . We know from the Schrieffer-Wolff transformation that for  $U = U_{12} \gg D$ , the model in this regime is equivalent to an SU(4) Coqblin-Schrieffer model.<sup>6,33,34</sup> The condition that  $U = U_{12}$  is not strictly required in this regime for the mapping to hold provided both  $U \gg D$  and  $U_{12} \gg D$ . The question arises, therefore, as to whether the mapping could still hold for  $U_{12} < U$  over a range with  $U < D$ . We test this possibility by calculating  $\tilde{U}_{12}/\tilde{U}$  as a function of  $U_{12}/U$  for  $\varepsilon_d = -3\pi\Gamma$ . The results are shown in Fig. 12 for  $U/D = 0.12, 0.2, 0.5, 1, 10, 100$ . We see that for values of  $U < D$ , we get the SU(4) symmetric case with  $\tilde{U}_{12}/\tilde{U} = 1$  only if  $U_{12} = U$ . For  $U/D > 1$  and  $U_{12} > D$  we do find SU(4) symmetry with  $\tilde{U}_{12}/\tilde{U} = 1$  in complete agreement with the result from the Schrieffer-Wolff transformation.

#### APPENDIX D: DIFFERENTIAL CONDUCTANCE IN A FIELD

If a magnetic field is applied to suppress the spin excitations in large fields the conductance should correspond to the SU(2) Kondo regime for the pseudospins. In Fig. 13, we plot the linear conductance in the individual spin channels,  $G_u$  (spin up) and  $G_d$  (spin down), and the total  $G_{\text{tot}}$ , as a function of applied magnetic field (log scale) using the results shown in Fig. 6.

The conductance in zero field is that at the degeneracy point where  $G_u/g_i G_0 = G_d/g_i G_0 = 0.5$ , and as the magnetic field is increased conductance due to the down excitations

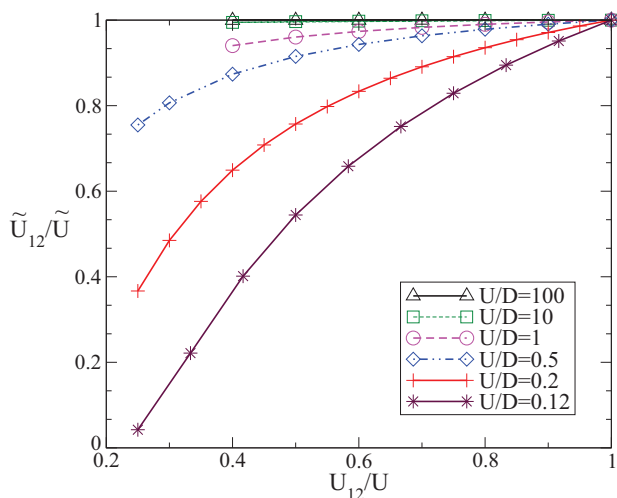


FIG. 12. (Color online) A plot of  $\tilde{U}_{12}/\tilde{U}$  as a function of  $U_{12}/U$  for  $\varepsilon_d = -3\pi\Gamma$  and  $U/D = 0.12, 0.2, 0.5, 1, 10, 100$ .

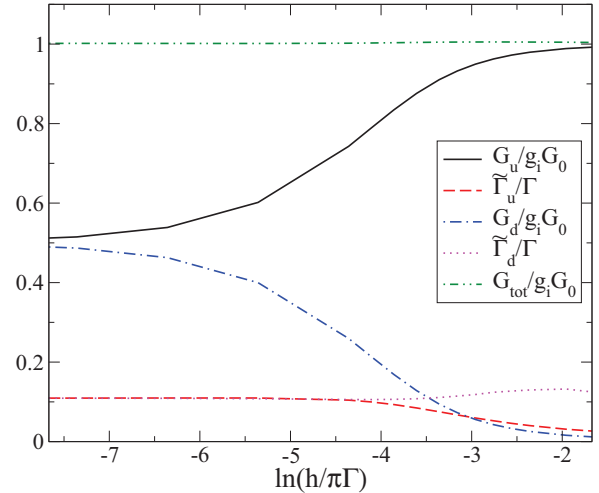


FIG. 13. (Color online) A plot of the linear conductance of the up and down electrons,  $G_u/g_i G_0$  and  $G_d/g_i G_0$ , and their sum  $G_{\text{tot}}/g_i G_0$ , as a function of  $\ln(h/\pi\Gamma)$  together with the renormalized resonance widths,  $\tilde{\Gamma}_u/\Gamma$  and  $\tilde{\Gamma}_d/\Gamma$ , for the results shown in Fig. 6.

is suppressed and that due to the up electrons increased and approaches that for the SU(2) Kondo model. Hence, in this large magnetic field case we observe spin polarized conductance through the dots which can reach the unitary limit. The renormalized resonance widths of the up and down electrons,  $\tilde{\Gamma}_u$ , and  $\tilde{\Gamma}_d$ , are shown in the same figure, that for the up electrons narrowing significantly with increase of field while that for the down electrons broadens slightly. In this situation where we have treated the dots as identical the total conductance is independent of the magnetic field. This means that any deviation from this result would give information on the differences between the dots and the couplings to their respective baths.

In Fig. 14, we show the conductances of the individual dots on suppressing the pseudospin excitations by changing the levels on the individual dots such that  $\bar{\varepsilon}_d$  is held constant so as to induce a pseudospin field  $h_{\text{ps}}$ .

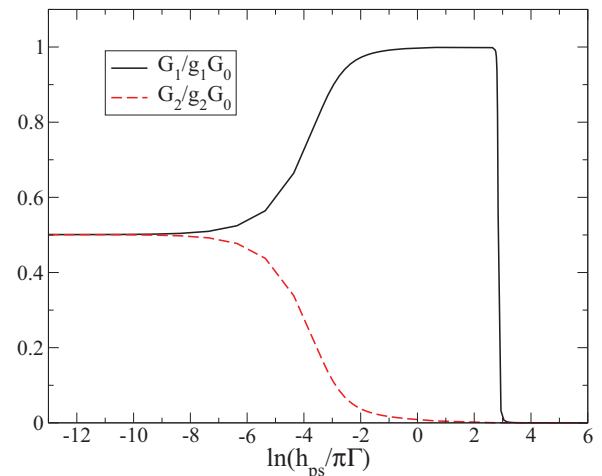


FIG. 14. (Color online) A plot of the linear conductances  $G_1/g_1 G_0$  and  $G_2/g_2 G_0$  as a function of  $\ln(h_{\text{ps}}/\pi\Gamma)$  for the parameters shown in Fig. 7.

The results are for the parameter set given in Fig. 7. As the pseudospin field is increased from the degeneracy point ( $\tilde{\epsilon}_d = \tilde{\Gamma}$ ,  $n_{d,1} = n_{d,2} = 0.5$ ) there is a crossover such that the occupation number on dot 1 increases,  $n_{d,1} \rightarrow 1$ , and that on dots 2 decreases,  $n_{d,2} \rightarrow 0$ . Over this range the conductance on dot 1 approaches that of an SU(2) Kondo model due to the remaining spin degrees of freedom, while that on dot 2 tends to zero. However, when the pseudospin field reaches values such that both spin states on dot 1 are occupied and  $n_{d,1} \rightarrow 2$ , the conductance on dot 1 shows a very rapid crossover such that  $G_1 \rightarrow 0$ .

#### APPENDIX E: DIFFERENTIAL CONDUCTANCE AT FINITE TEMPERATURE: TEST CASE

Here we test the approximation for the temperature dependence of conductance against the NRG results in Fig. 2 in the paper by Merker *et al.*<sup>39</sup> for the single-impurity Anderson model. The results of this comparison are shown in Fig. 15 for  $D = 1$ ,  $\Lambda = 1.7$ , and  $\eta = 0.55$ .

It can be seen that in the most strongly correlated case corresponding to the particle-hole symmetric model ( $T_0 = T_K$ ) the agreement is excellent up to  $T = 2T_K$  and is a good approximation for  $T < 150T_K$ . In all three NRG results there is a regime where the conductance increases with temperature before falling off again at higher temperatures resulting in a peak. The small peak at higher temperatures for the particle-hole symmetric case is due to the influence of the atomic peaks at  $\omega = \pm U/2$ ; this is not seen in the results using quasiparticle approximation for the spectral density as the latter does not include these atomic features. In the less correlated cases away from particle-hole symmetry the overall agreement is very good and reproduces the peaks seen in the accurate NRG calculations. The temperature dependence of the renormalized parameters plays a more

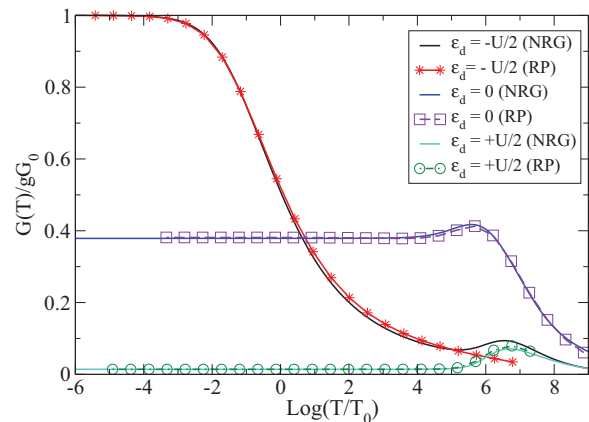


FIG. 15. (Color online) The results for linear conductances  $G(T)/gG_0$  as a function of  $\ln(T/T_0)$  for the single-impurity Anderson model for  $U = 16\Gamma$  and  $\epsilon_d = -U/2, 0, U/2$  given by Merker *et al.* (Ref. 39) (NRG) compared with the approximate results based on temperature-dependent renormalized parameters (RP). The value of  $T_0$  is defined by  $\chi(0) = 1/4T_0$ , where  $\chi(0)$  is the zero-temperature impurity susceptibility. Note that the particle-hole symmetric case  $\epsilon_d = -U/2$  is in the localized limit where  $T_0 = T_K$ .

important role in the more correlated cases. In the weakly correlated case  $\epsilon_d = U/2$  the temperature dependence of the parameters plays no role and the peak in the higher temperature regime is due to the location of the quasiparticle peak in the spectral density. The position of the peak for  $\epsilon_d = 0$  is also due to the location of the quasiparticle peak in the spectral density but its height is reduced by the temperature dependence of the parameters. We conclude that the main features in the temperature dependence of the differential conductance can be understood in terms Eq. (25) using the quasiparticle density of states with temperature-dependent parameters.

<sup>1</sup>W. G. van der Wiel, S. De Franceschi, J. M. Elzerman, T. Fujisawa, S. Tarucha, and L. P. Kouwenhoven, *Rev. Mod. Phys.* **75**, 1 (2002).

<sup>2</sup>T. Pohjola, H. Schoeller, and G. Schön, *Europhys. Lett.* **54**, 241 (2001).

<sup>3</sup>L. Borda, G. Zaránd, W. Hofstetter, B. I. Halperin, and J. von Delft, *Phys. Rev. Lett.* **90**, 026602 (2003).

<sup>4</sup>R. López, D. Sánchez, M. Lee, M.-S. Choi, P. Simon, and K. Le Hur, *Phys. Rev. B* **71**, 115312 (2005).

<sup>5</sup>M. R. Galpin, D. E. Logan, and H. R. Krishnamurthy, *Phys. Rev. Lett.* **94**, 186406 (2005).

<sup>6</sup>A. K. Mitchell, M. R. Galpin, and D. E. Logan, *Europhys. Lett.* **76**, 95 (2006).

<sup>7</sup>T. Choi, I. Shorubalko, S. Gustavsson, S. Schön, and K. Ensslin, *New J. Phys.* **11**, 013005 (2009).

<sup>8</sup>A. M. Chang and J. C. Chen, *Rep. Prog. Phys.* **72**, 096501 (2009).

<sup>9</sup>Y. Okazaki, S. Sasaki, and K. Muraki, *Phys. Rev. B* **84**, 161305 (2011).

<sup>10</sup>G. C. Tettamanzi, J. Verduijn, G. P. Lansbergen, M. Blaauboer, M. J. Calderón, R. Aguado, and S. Rogge, *Phys. Rev. Lett.* **108**, 046803 (2012).

<sup>11</sup>D. Goldhaber-Gordon, H. Shtrikman, D. Mahalu, D. Abusch-Magder, U. Meirav, and M. A. Kastner, *Nature (London)* **391**, 156 (1998).

<sup>12</sup>S. M. Cronenwett, T. H. Oosterkamp, and L. P. Kouwenhoven, *Science* **281**, 540 (1998).

<sup>13</sup>W. G. van der Wiel, S. D. Franceschi, T. Fujisawa, J. M. Elzerman, S. Tarucha, and L. P. Kouwenhoven, *Science* **289**, 2105 (2000).

<sup>14</sup>A. Kogan, S. Amasha, D. Goldhaber-Gordon, G. Granger, M. A. Kastner, and H. Shtrikman, *Phys. Rev. Lett.* **93**, 166602 (2004).

<sup>15</sup>S. Amasha, I. J. Gelfand, M. A. Kastner, and A. Kogan, *Phys. Rev. B* **72**, 045308 (2005).

<sup>16</sup>K. Le Hur and P. Simon, *Phys. Rev. B* **67**, 201308 (2003).

<sup>17</sup>K. Le Hur, P. Simon, and L. Borda, *Phys. Rev. B* **69**, 045326 (2004).

<sup>18</sup>G. Zaránd, *Philos. Mag.* **86**, 2043 (2006).

<sup>19</sup>K. Le Hur, P. Simon, and D. Loss, *Phys. Rev. B* **75**, 035332 (2007).

<sup>20</sup>A. Hübel, K. Held, J. Weis, and K. v. Klitzing, *Phys. Rev. Lett.* **101**, 186804 (2008).

<sup>21</sup>S. Amasha, A. J. Keller, I. G. Rau, A. Carmi, J. A. Katine, H. Shtrikman, Y. Oreg, and D. Goldhaber-Gordon, *Phys. Rev. Lett.* **110**, 046604 (2013).

- <sup>22</sup>A. J. Keller, S. Amasha, I. Weymann, C. P. Moca, I. G. Rau, J. A. Katine, H. Shtrikman, G. Zaránd, and D. Goldhaber-Gordon, *Nat. Phys.*, doi:[10.1038/nphys2844](https://doi.org/10.1038/nphys2844), [arXiv:1306.6326v1](https://arxiv.org/abs/1306.6326v1).
- <sup>23</sup>K. Wilson, *Rev. Mod. Phys.* **47**, 773 (1975).
- <sup>24</sup>R. Bulla, T. Costi, and T. Pruschke, *Rev. Mod. Phys.* **80**, 395 (2008).
- <sup>25</sup>A. C. Hewson, A. Oguri, and D. Meyer, *Eur. Phys. J. B* **40**, 177 (2004).
- <sup>26</sup>Y. Nishikawa, D. J. G. Crow, and A. C. Hewson, *Phys. Rev. B* **86**, 125134 (2012).
- <sup>27</sup>A. C. Hewson, *J. Phys. Soc. Jpn.* **74**, 8 (2005).
- <sup>28</sup>A. C. Hewson, J. Bauer, and W. Koller, *Phys. Rev. B* **73**, 045117 (2006).
- <sup>29</sup>A. C. Hewson, *Phys. Rev. Lett.* **70**, 4007 (1993).
- <sup>30</sup>A. C. Hewson, *J. Phys.: Condens. Matter* **13**, 10011 (2001).
- <sup>31</sup>A. C. Hewson, *J. Phys.: Condens. Matter* **18**, 1815 (2006).
- <sup>32</sup>Y. Nishikawa, D. J. G. Crow, and A. C. Hewson, *Phys. Rev. B* **82**, 245109 (2010).
- <sup>33</sup>A. C. Hewson, *The Kondo Problem to Heavy Fermions* (Cambridge University Press, Cambridge, 1993).
- <sup>34</sup>Y. Nishikawa, D. J. G. Crow, and A. C. Hewson, *Phys. Rev. B* **82**, 115123 (2010).
- <sup>35</sup>J. Bauer and A. C. Hewson, *Phys. Rev. B* **76**, 035119 (2007).
- <sup>36</sup>L. Tosi, P. Roura-Bas, and A. A. Aligia, *Phys. Rev. B* **88**, 235427 (2013).
- <sup>37</sup>Y. Meir and N. S. Wingreen, *Phys. Rev. Lett.* **68**, 2512 (1992).
- <sup>38</sup>H. R. Krishna-murthy, J. W. Wilkins, and K. G. Wilson, *Phys. Rev. B* **21**, 1003 (1980).
- <sup>39</sup>L. Merker, S. Kirchner, E. Muñoz, and T. A. Costi, *Phys. Rev. B* **87**, 165132 (2013).
- <sup>40</sup>S. Donsa, S. Andergassen, and K. Held, [arXiv:1308.4882](https://arxiv.org/abs/1308.4882).
- <sup>41</sup>D. Feinberg and P. Simon, *Appl. Phys. Lett.* **85**, 1846 (2004).
- <sup>42</sup>E. Vernek, C. Busser, E. Anda, A. Feiguin, and G. Martins, [arXiv:1308.4746](https://arxiv.org/abs/1308.4746).
- <sup>43</sup>A. Oguri, *J. Phys. Soc. Jpn.* **71**, 2969 (2002).
- <sup>44</sup>A. Oguri, *J. Phys. Soc. Jpn.* **74**, 110 (2005).
- <sup>45</sup>A. C. Hewson, J. Bauer, and A. Oguri, *J. Phys.: Condens. Matter* **17**, 5413 (2005).
- <sup>46</sup>H. R. Krishna-murthy, J. W. Wilkins, and K. G. Wilson, *Phys. Rev. B* **21**, 1044 (1980).
- <sup>47</sup>P. W. Anderson, *J. Phys. C* **3**, 2436 (1970).